Vol: 2
Issue: 1
March, 2022

ADVANCED LIDAR

Online ISSN: 2791-8572

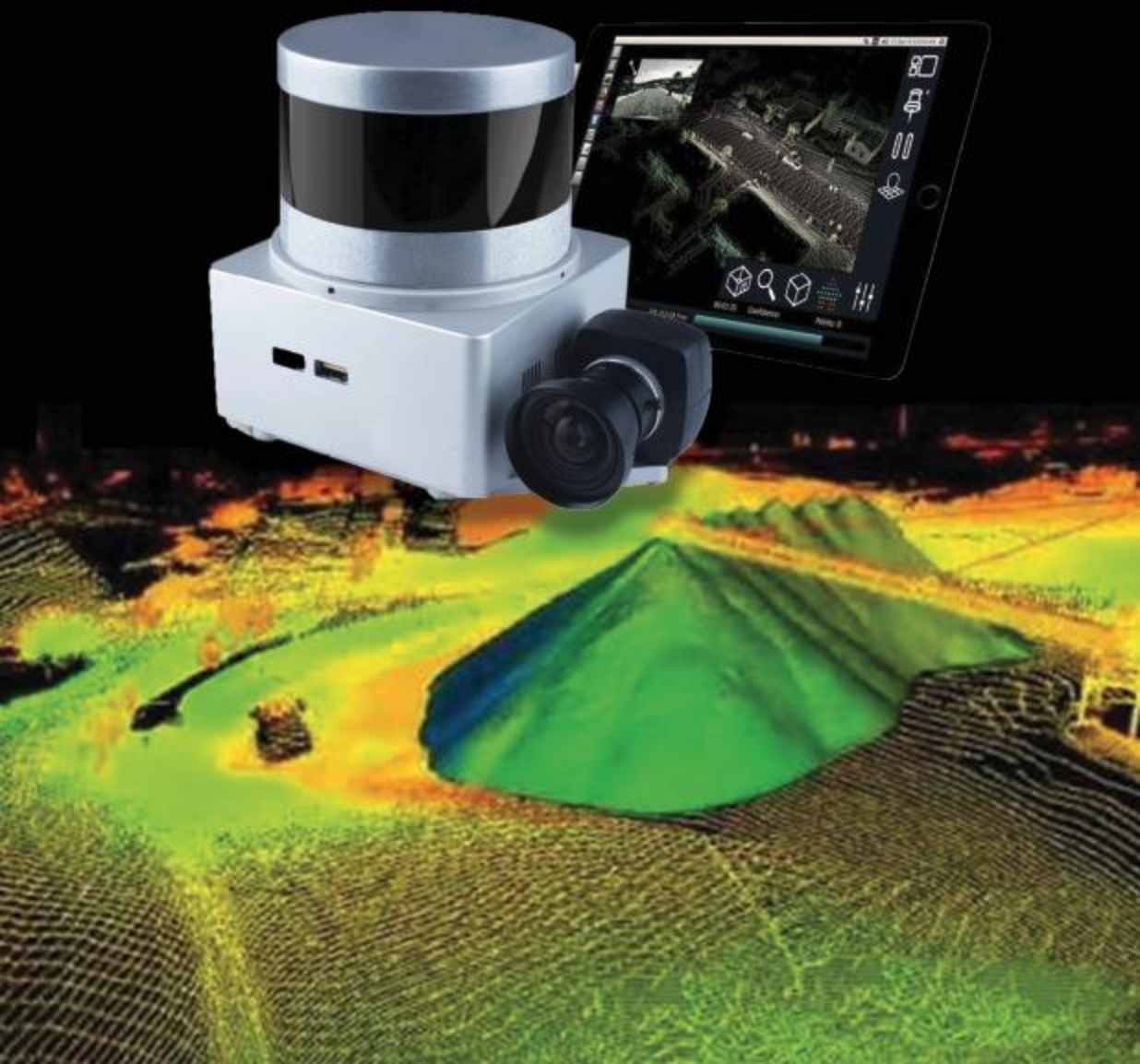

Advanced LiDAR

About Journal

The Advanced LiDAR is a peer-reviewed journal that publishes studies on LiDAR technology development, use, and earth sciences and is scanned in International Indexes and Databases. The journal, LiDAR Systems, and LiDAR Autonom Systems, etc. focuses on the design and applications of LiDAR, including.

Aim & Scope

Turkish Journal of LiDAR,

- To present international developments in the use of terrestrial, wearable, UAV, air, and mobile LiDAR to the information of scientists interested in the fields of Map, Geology, Environment, Mining, Urban Planning, Agriculture, archeology, and architecture.
- To provide an easily accessible and wide-ranging discussion environment that will strengthen and accelerate the sharing of knowledge and experience between scientists, researchers, engineers, and other practitioners who are involved in direct or indirect activities with the following topics.
- To contribute to the initiation and development of inter-institutional cooperation with LiDAR technology, which is of great importance in solving problems related to professional developments that can play a role in technological and economic development in the world and in Turkey.

The scope of Turkish Journal of LiDAR;

- ✓ Basic LiDAR Applications,
- ✓ LiDAR Platforms
- ✓ Terrestrial LiDAR Applications
- ✓ Hand-Held LiDAR Applications
- ✓ Mobile LiDAR Applications
- ✓ Wearable LiDAR Applications
- ✓ Air LiDAR Applications
- ✓ UAV LiDAR Applications
- ✓ LiDAR Autonomous Systems
- ✓ Augmented Reality and virtual reality (VR) applications with LiDAR,
- ✓ Geographical Information Systems integration with LiDAR data,
- ✓ Documentation Studies with LiDAR
- ✓ Industrial measurements with LiDAR,
- ✓ Deformation and Landslide Measurements with LiDAR,
- ✓ Mining Measurements with LiDAR,
- ✓ Urbanism and Transportation Planning Studies with LiDAR,
- ✓ Agricultural Applications with LiDAR,
- ✓ Hydrographic Applications with LiDAR,
- ✓ 3D modeling with LiDAR
- ✓ All multidisciplinary studies conducted with LiDAR,

Publication frequency Biannual

WEB http://publish.mersin.edu.tr/index.php/lidar

Contact alid@mersin.edu.tr / ayasinyigit@mersin.edu.tr

Advanced LiDAR

EDITOR in CHIEF

Prof. Dr. Murat YAKAR
Mersin University, Department of Geomatics Engineering (myakar@mersin.edu.tr) Mersin

EDITOR

Asst. Prof. Ali ULVİ
Mersin University, Institute of Science and Technology / Remote Sensing and Geographic Information Systems, aliulvi@mersin.edu.tr), Mersin

EDITORIAL BOARD

- ***Prof. Dr. Hacı Murat YILMAZ,*** Aksaray University ***hmuraty@gmail.com,***
- ***Assoc. Prof. Dr. Murat UYSAL,*** Afyon Kocatepe University ***muysal@aku.edu.tr,***
- ***Assist. Prof. Dr. Bilgehan KEKEÇ,*** Konya Technical University ***kekec@ktu.edu.tr,***
- ***Dr. Nizar POLAT,*** Harran University ***nizarpolat@harran.edu.tr,***

Dr. Mustafa Zeybek, Selçuk University ***mzeybek@selcuk.edu.tr***

ADVISORY BOARD

- ***Prof. Dr. İbrahim YILMAZ,*** ***iyilmaz@aku.edu.tr,*** Afyon Kocatepe University
- ***Dr. Alper AKAR,*** Erzincan Binali Yıldırım University, ***alperakar@erzincan.edu.tr,***
- ***Dr. Özlem AKAR,*** Erzincan Binali Yıldırım University ***oakar@erzincan.edu.tr,***
- ***Dr. Mehmet Ali DERELİ,*** Giresun University ***madereli@gmail.com*** Giresun University
- ***Dr. Hayri ULVİ,*** Gazi University ***hayriulvi@gmail.com,***
- ***Dr. Resul ÇÖMERT,*** ***rcomert@gumushane.edu.tr,*** Gümüşhane University

Language Editors

Res. Asst. Halil İbrahim ŞENOL, Harran University, ***hsenol@harran.edu.tr***

Mizanpaj

Res. Asst. Abdurahman Yasin YİĞİT, Mersin University, ***ayasinyigit@mersin.edu.tr***

Res. Asst. Yunus KAYA, Harran University, ***yunuskaya@harran.edu.tr***

Eng. Seda Nur Gamze HAMAL Mersin University, ***sedanurgamzehamal@gmail.com***

Advanced LiDAR
Volume *2*
Issue *1* *March, 2022*

Contents

Research Articles;*

Research Article

2022: 2(1); 01-09

Advanced LiDAR

http://publish.mersin.edu.tr/index.php/lidar/index

e-ISSN 2791-8572

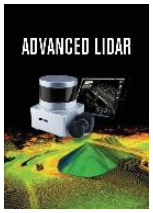

Evaluation of Machine Learning Classifiers for 3D Mobile LiDAR Point Cloud Classification Using Different Neighborhood Search Methods

Mahmoud Mohamed*[1], Salem Morsy[2], Adel El-Shazly[2]

[1]*Fayoum University, Faculty of Engineering, Civil Engineering Department, Eqypt*
[2]*Cairo University, Faculty of Engineering, Public Works Department, Eqypt*

Keywords
Mobile LiDAR,
Road Features,
Machine Learning,
Neighborhood Selection.

ABSTRACT

Mobile LiDAR systems are distinguished with large and highly accurate point clouds data acquisition for road environments. Road features extraction is becoming one of the most important applications of LiDAR point cloud, and is used largely in road maintenance and autonomous driving vehicles. The main step in Mobile LiDAR processing is point classification This classification relies on the geometric definition of the points and their surroundings, as well as the classification methods used. The neighbors of each point is helpful to find more meaningful information than the raw coordinates. On the other hand, machine learning algorithms have proved their efficiency in LiDAR point cloud classification. This research compares results of using three machine learning classifiers, namely Random Forest, Gaussian Naïve Bayes, and Quadratic Discriminate Analysis along with using three neighborhood search methods, namely k nearest neighbors, spherical and cylindrical. A part of the pre-labelled benchmark dataset (Paris Lille 3D) with about 98 million points was tested. Results showed that the using Random Forest classifer with the cylindirical neighborhood search method acheived the highest overall accuracy of 92.39%.

1. INTRODUCTION

Laser scanning systems are widely used as remote sensing techniques based on Light Detection and Ranging (LiDAR). These systems have been involved into surveying market, providing high accuracy measurements as well as efficient data collection, especially in the 3-Dimensional environments. LiDAR technology is non-contact active measuring to get information of the scanned 3D surfaces with less dependence on illuminations. LiDAR scanning systems have also the ability to record point cloud actively and precisely at a high speed in real time (Pu & Vosselman, 2009). The rapid acquisition of high 3D information of objects has been more realized due to the most recent advances in the technology (Yu et al., 2014).

3D point clouds could be obtained in precise format using one of main laser scanning systems types; Airborne, Terrestrial or Mobile (Hyyppä et al., 2013). In the past decades, the market has a high demand for utilizing data acquired from Mobile Laser Scanning (MLS) systems. The applicability of MLS from moving platforms allows for the complete coverage of complex urban environments. 3D point data acquired from MLS systems are distinguished with their high accuracy level and points density, with an average of about 1000-2000 pts./m^2. The bottleneck in any work is the transmission from field data acquisition to the processing step with a large amount of data that sometimes represent hindrances and thus need to be managed effectively. As MLS systems often provide high dense point clouds, their processing will be labor intensive (Guarnieria et al., 2009), and may last for days to handle those data that were collected in a very short time.

The MLS system consists mainly of a laser scanning sensor, global navigation satellite system (GNSS) and inertial navigation system (INS) unit. Laser scanning sensor is responsible for the emission of laser beams and reception the reflected rays. Because the laser beams have a constant speed (i.e., speed of light, S) and with measuring the time elapsed, t, from the emission and reception of the beams using a precise interval timer, the distance between the sensor and the object can be measured according to the first Newton's rule Equation (1). It should be noted that the distance, D, calculated using Newton's rule is twice the distance between the system and any measured object.

$$D = S*t \quad (1)$$

*Corresponding Author

*(maa58@fayoum.edu.eg) ORCID ID 0000-0002-8690-3192
(morsy@eng.cu.edu.eg) ORCID ID 0000-0002-1683-2050
(adel.shazly@eng.cu.edu.eg) ORCID ID 0000-0003-4332-9386

Cite this;

Mohamed M., Morsy, S. & Shazly, A. (2022). Evaluation of machine learning classifiers for 3D mobile LiDAR point cloud classification using different neighborhood search methods. Advanced LiDAR, 2(1), 01-09.

Research Article

Accepted: 20/03/2022

GNSS is another main component in MLS system. It is used to determine the accurate position of the system instantly. This would help to geo-reference any measured object to the global system supported by the GNSS unit. INS has a role to determine the system values of roll, pitch and heading, which helps to determine the relative position between any scanned object and the system at the measurement time.

There are additional components that could be mounted on the system such as digital cameras and distance measurement instruments (DMIs). Digital cameras are optional choice, and their videos/images are not included in the process of LiDAR data except for some methods of features extraction or 3D reconstruction that integrates the LiDAR point clouds with imagery. DMIs are used to continuously measure the distance passed by the vehicle. This helps in case of the integration with INS to determine the position of the whole system in case of the disability of the GNSS unit due to instant interruptions.

The development in MLS systems is scaled with two main topics: how much the accuracy of collected data is increased, and the availability of developing software packages that make the processing of the point cloud easier, faster and more precise. The former is improved through the MLS system itself and its internal components, either hardware or software. The latter is divided into three main steps and they are improved individually. The three steps are removal of the outliers within the dataset, detection of the required features and the modeling of the extracted features to produce CAD models. The features' detection step is still under continuous development for the purpose of evaluating its level of automation and identifying different features simultaneously.

Automatic 3D point clouds processing is an important topic in most cases related to remote sensing, photogrammetry and computer vision because of the time consumed and cost of user-assisted analysis. Current researches aim to decrease the human involvement in the point clouds processing. In the past years, machine learning classifiers have had a great contribution to 3D point clouds processing, and covered all types of LiDAR systems; airborne, terrestrial, or mobile (Chehata et al., 2009; Mohamed et al., 2021a; Nguyen et al., 2020).

Machine learning (ML) is a subfield related to computer science that is mainly concerned with constructing useful algorithms which rely on a collection of given examples of some phenomenon. ML can also be defined as the process of solving a practical problem. This is conducted through gathering required dataset, algorithmically build a statistical model based on that dataset, and the statistical model is somehow expected to solve the practical problem (Burkov, 2019).

Supervised machine learning is one of ML algorithms that uses the dataset to produce a model which takes a feature vector x as input and output information and allows deducing the label for this feature vector (Burkov, 2019). There are various supervised learning algorithms which differ according to their mathematical definition such as k Nearest Neighbor, Logistic Regression, Naïve Bayes, Discriminant Analysis, Decision Tree, Random Forest, Support Vector Machine, and Neural Network. Figure 1 shows an example of a supervised learning algorithm whereas it predicts a yellow edge boundary between two classes (Red and Blue classes) according to inputs attributes of X and Y.

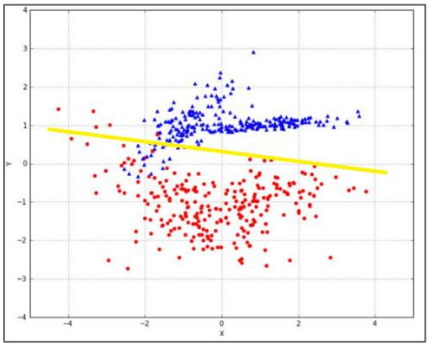

Figure 1. An example of a supervised learning algorithm (Bonaccorso, 2017)

1.1. Mobile LiDAR Data Classification Using Machine Learning

ML classifiers require input data that are distinguishable to categorize each class. However, MLS point cloud in its raw format consisting of 3D coordinates (i.e., X, Y and Z) and sometimes intensity values are not sufficient for ML to differentiate between different classes. Coordinates are meaningless for ML classifiers except for Z coordinate which may somehow be used to extract some classes such as ground (i.e., the lowest points within any point cloud dataset). In addition, intensity values may differ for points of same class according to weather conditions or how far the point from the sensor is.

Due to the ability of ML classifiers to distinguish between multiple classes, most researches that applied ML classifiers aimed at multi-classification (Hackel et al., 2016; Mohamed et al., 2021b; Weinmann et al., 2013), but there were also some researches that focused on one class such as rail track detection in (Elberink et al., 2013) out of all other classes. Generally, the classification process is divided into three steps; neighborhood search method, features extraction and ML classifier.

Neighborhood search method is defined as the predetermined scale around each point. The neighborhood may take various types according to the geometric definition such as K nearest neighbors (KNN), spherical and cylindrical neighborhoods as illustrated in Figure 2. KNN method is defined as the most nearest k number of points to the point of interest x according to the Euclidean distance (Linsen & Prautzsch, 2001). The determination of how much k neighbors has been studied in (Hackel et al., 2016; Weinmann et al., 2013) where a fixed number of points for all points was applied. Others applied a different and changing k number for each individual point according to a specific condition (Demantké et al., 2011; Weinmann et al., 2014; Weinmann, Jutzi, et al., 2015; Weinmann, Urban, et al., 2015).

Spherical neighborhood method of point x is defined by a sphere with a radius r and centered with the point of interest x (Lee & Schenk, 2002). Cylindrical neighborhood is determined by the cylinder centered

with the point of interest x, and its neighbors are all points within that cylinder. The cylinder is defined with a 2D radius r and its height may be a specific value above and below the point of interest, or may be infinite (Filin & Pfeifer, 2005). This neighborhood step allows getting most of common used features in the classification process, from Eigenvalues and Eigenvectors derived from their covariance matrix, or from heights of the neighborhood points.

Spherical and cylindrical neighborhoods have not been widely used in 3D point neighborhood search. (Li et al., 2021) used a spherical neighborhood method around the points within 0.5 m radius. (Weinmann et al., 2017) used the spherical and cylindrical neighborhood in a comparison with KNN in its two ways; fixed and optimal k value. They used four individual neighborhoods, cylindrical with 1.0 m radius, spherical with 1.0 m radius, and two KNN with k = 50 and optimal k of each point according to Eigen entropy defined in (Weinmann, Jutzi, et al., 2015). Other approaches proposed a multi-scale neighborhood with different features extracted from different neighborhoods at the same time. (Hackel et al., 2016) proposed a multi-scale neighborhood using (k = 10) of KNN. (Blomley et al., 2016) used a cylindrical multi-scale neighborhood of radius (1m, 2m, 3m, and 5m) as well as KNN with the optimal value of k according to the Eigen entropy defined by (Weinmann et al., 2014) with the normalized Eigenvalues. (Zheng et al., 2017) used a cylindrical neighborhood with radius r_C = 0.25 m, (Zheng et al., 2018) used other values (0.45, 0.6, 0.75, 0.9, 1.05) m, but without any significant effect on the results.

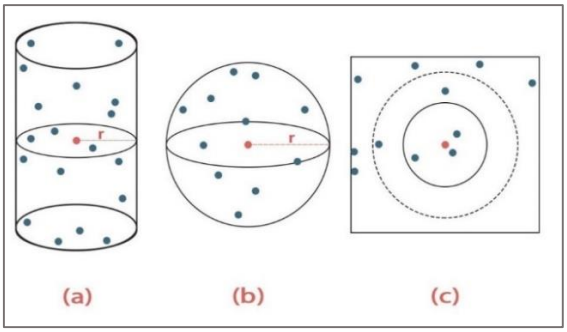

Figure 2. A definition of neighborhood is presented where (a) the cylindrical neighborhood, (b) the spherical neighborhood, and (c) the k nearest neighborhood. Also, the point in red is the point of interest, and r is the predefined radius for the neighborhood.

The second step in the classification process of XYZ point cloud is to extract much more meaningful information from those data than the XYZ coordinates. One of the most used set of features are covariance features, those covariance features are derived from the covariance matrix of each point's neighborhood (Pauly et al., 2003; West et al., 2004). Those features are computed using the Eigenvalues $(\lambda_1, \lambda_2, and\ \lambda_3)$ of the covariance matrix. According to (Weinmann et al., 2013), for a linear (1D) structure; λ_1 is the largest between the three Eigenvalues. For a (2D) planar structure, $(\lambda_1\ and\ \lambda_2)$ are much larger than λ_3, while a (3D) volumetric structure has similar Eigenvalues (Dittrich et al., 2017). In (Weinmann et al., 2014; Weinmann, Jutzi, et al., 2015; Weinmann, Urban, et al., 2015), they replaced the Eigenvalues with their normalized values $(e_1, e_2, and\ e_3)$ where $(e_i = \lambda_i / \sum_{i=1} \lambda_i)$.

Another common set of features is the moment features which implemented previously is (Hackel et al., 2016), those features were derived from the dot product of the coordinates' array and the Eigenvectors of the covariance matrix. (Demantké et al., 2011; Hackel et al., 2016) had also added another feature which may be considered as a covariance feature, namely verticality. This feature was derived from the vertical component of the normal vector. The Eigenvalues were used in a previous work of (Chehata et al., 2009) and (Wang et al., 2020), where the Eigenvalues were added as features in addition to waveform features.

The last set of features is the height features. These features are derived from the Z-coordinate of the points within the local neighborhood of each point. (Weinmann et al., 2013) used the neighborhood of each point to calculate the standard deviation of the points' heights as well as the maximum difference of the heights. (Hackel et al., 2016) also used the heights of the points to calculate the maximum height difference, the maximum height below the point of interest, and the maximum height above the point of interest. Another height feature is the height above ground, but was used in Airborne LiDAR Scanning classification. The definition of the ground was set to the lowest point within a cylindrical neighborhood according to (Chehata et al., 2009) and (Mallet et al., 2011). They used a cylindrical neighborhood around the point of interest with a 15 m and 20 m radius, respectively.

1.2. Research Objectives

This article aims to investigate the effectiveness of machine leaning classifiers for the sake of road features extraction, also the importance of choosing appropriate neighborhood method and its direct impact on the classification results. The two main objectives of this research are 1) evaluate the effectiveness of using three neighborhood selection methods for MLS data and 2) evaluate the application of three machine learning algorithms for MLS data classification.

2. METHOD

The methodology of this research is divided into four stages as shown in Figure 3. First, the pre-processing stage which contains data subsampling and data slicing. Second, the neighborhood search method to find the neighbors of each point, it includes three alternatives (section 2.2). Third, geometric features extraction that will replace the XYZ coordinates as input to ML classifiers. Finally, three ML classifiers are applied to learn and classify the dataset (section 2.4).

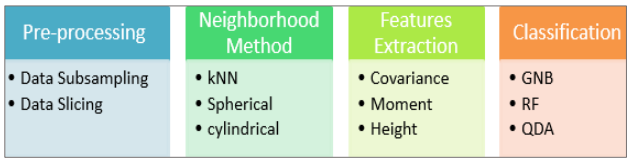

Figure 3. 3D point clouds classification workflow

2.1. Pre-processing Stage

2.1.1. Data Subsampling

Due to the high points' density of MLS systems, data processing means time. Hence, different researches suggested various scenarios for the reduction of the dataset. For instance, (Zheng et al., 2017, 2018) removed the ground points as their research's aim was to classify non-ground points. Another research, (Weinmann et al., 2014), removed any class with points' count less than 0.05% of the whole dataset. However, this could result in losing significant information of removed points. On the other hand, the huge amount of MLS point cloud may be more than the amount of information required to detect the urban road objects. Thus, removal of some points in a specific manner would improve the classification processing time, which is a major evaluation factor of any method. This is applicable if the reduction in the dataset does not harm the information and the classification results are acceptable compared to results of the whole dataset (Mohamed et al., 2021a).

Reducing the dataset may be through variant manners according to the organization of the dataset and the differences in the point density. As much as the dataset is organized and equally distributed, the point reduction may be more applicable by a high percentage. We used the dame subsampling method implemented in (Mohamed et al., 2021a), the subsampling was by the minimum spacing between points, and the reduction in the dataset was by about the half but without low reduction in the results, whereas the overall accuracy was 92.39% and 90.26% for the full and subsampled datasets.

2.1.2. Data Slicing

Figure 4 shows the effect of slicing on finding the neighbors of any point within the black points on the left side of the dataset. It has no meaning to search for neighbors within the whole dataset including the white points as there is no way to have neighbors from the white points. Therefore, if the search of the neighborhood of any point is within a small slice of the dataset, the processing time will be more efficient. Slicing of the dataset could be by distance or equal number of points along the dataset. In this research, we divided the dataset into slices with same amount of points along the road and added two overlaps before and after each slice to best calculate the neighbors of edge points.

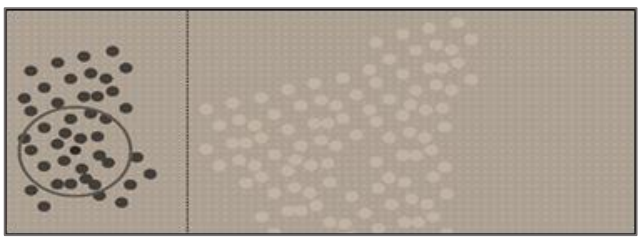

Figure 4. Data slicing for neighborhood search

The disadvantage in the slicing concept is that points on the edge will find their neighbors from one side only and this may affect the results. The more slices we have, the more edges we get, and hence the effect will be increased. In order to avoid this effect, each slice will be extended with an overlap from each edge to find the neighbors of the edge points effectively.

2.2. Neighborhood Search Stage

Neighborhood method is used to find the neighbors of any point and derive extract features from its surroundings. As aforementioned, there are three common types of neighborhood; KNN which is based on the Euclidian distance, and spherical and cylindrical neighborhoods which are based on a predefined radius. The choice between those three types depends on the uniformity and points' density in the used dataset. Searching by a fixed radius (i.e., spherical and cylindrical neighborhoods) in dataset with uniformly point density is usually suitable as it preserves the objects in a fixed geometry scale. However, the strongly varying point density requires a fixed number of points; hence, the KNN is an effective choice (Hackel et al., 2016).

K nearest neighborhood is determined by the nearest (k) points to the point of interest. The change in the number of k points by increasing or decreasing has a high linearly proportional relation with the processing time. In addition, it affects the classification results. More k points enhance the results but with more processing time. Spherical and cylindrical are determined by a radius r. A spherical neighborhood definition is the sphere with radius in 3D (r_{3D}) around the query point while cylindrical neighborhood is implemented in the 2D projection of points neglecting the height of points when searching for neighbors. The cylinder contains all points around the query point within 2D radius (r_{2D}) above and below the point.

2.3. Features Extraction Stage

For each point, we replace its coordinates with three sets of features; covariance, moment and height. Those features have had the most occurrence in previous researches. Figure 5 shows the structure of features extraction.

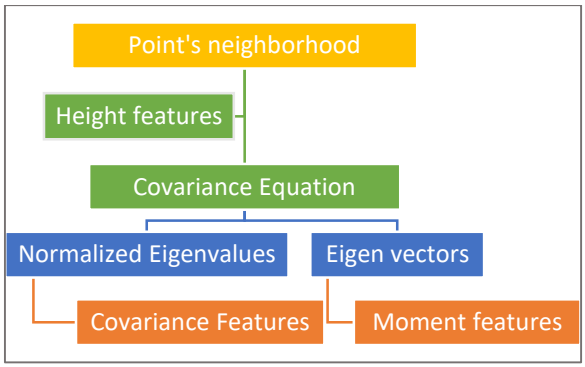

Figure 5. workflow of points' features extraction

A total of fifteen features are derived and used in this research as listed in Table 1. From the neighborhood of each point, the covariance matrix is constructed using the three coordinates' arrays as shown in Equation (2).

$$C = \frac{1}{n} \sum_{i \in N} (p_i - \bar{p})(p_i - \bar{p})^T \quad (2)$$

Where n is the number of points within the neighborhood of each point x, p_i is representing each point in the neighborhood, $\bar{p}$ is the centroid of n points in the neighborhood.

The result of the covariance matrix is three Eigenvalues $(\lambda_1, \lambda_2, and\ \lambda_3)$ and three Eigenvectors $(v_1, v_2, and\ v_3)$. The first subset of features, covariance features, are derived from the normalized Eigenvalues $(e_1, e_2, and\ e_3)$ where $e_i = \lambda_i/(\lambda_1 + \lambda_2 + \lambda_3)$. The covariance features are similar to what have been previously used in the research of (Weinmann, Urban, et al., 2015), except for the "Sum" feature that is derived from the summation of the three Eigenvalues, not the normalized ones. Another feature is added to the covariance set is the verticality which has been driven before in the research of (Demantké et al., 2011).

The second set of features (moment features) were first used in (Hackel et al., 2016). Those features are driven from the dot product of coordinates' arrays and the first two Eigenvectors. Those moment features are helpful in identifying the crease edges as well as occlusion boundaries. Height features are also used in this research. Those features include Δz: the max difference in height between all points within the neighborhood and σz: the standard deviation of z - coordinate of points.

Table 1. Geometric features

Items	Feature	Formula
Covariance features	L_λ: Linearity	$(e_1 - e_2)/e_1$
	P_λ: Planarity	$(e_2 - e_3)/e_1$
	S_λ: Scattering	e_3/e_1
	O_λ:Omni variance	$\sqrt[3]{e_1 e_2 e_3}$
	A_λ: Anisotropy	$(e_1 - e_3)/e_1$
	E_λ: Eigen entropy	$-\sum_{i=1}^{3} e_i \ln(e_i)$
	C_λ:Change of curvature	e_3
	$\sum_\lambda$: Sum	$\lambda_1 + \lambda_2 + \lambda_3$
	V: Verticality	$1 - \langle (0,0,1), v_3 \rangle$
Moment features	1st order, 1st axis (f11)	$\sum_{i \in p} \langle (p_i - p), v_1 \rangle$
	1st order, 2nd axis (f22)	$\sum_{i \in p} \langle (p_i - p), v_2 \rangle$
	2nd order, 1st axis (s11)	$\sum_{i \in p} \langle (p_i - p), v_1 \rangle^2$
	2nd order, 2nd axis (s22)	$\sum_{i \in p} \langle (p_i - p), v_2 \rangle^2$
Height Features	Δz	$Z_{max} - Z_{min}$
	σz	Standard deviation of z coordinate within the neighborhood

2.4. Machine Learning Classification Stage

Machine Learning has its ability to differentiate between different classes without any preprogramming. The results of any classification vary with respect to different classifiers and their suitability with the used dataset and given features. Three ML classifiers are evaluated in this research, including Random forest (RF), Gaussian Naïve Bayes (GNB), and Quadratic Discriminate Analysis (QDA).

2.4.1. Random Forest

RF classifier is an ensemble algorithm containing multiple tree decisions (Breiman, 2001). It combines multiple weak learners for the sake of a stronger one (Weinmann, Urban, et al., 2015). For each decision tree, the classifier makes nested relations between the input features and the output class according to specific conditions in the inputs. The more estimators (decision tress) are, the better results will be but with an increase in processing time. The optimization of best fitted RF model depends on various parameters of the algorithm that should be well tuned. In addition to the number of trees (estimators), there are other important parameters such as 'max_depth' and 'min_samples_split' parameters, both determine how far each tree will go down.

The mechanism of RF is simplified as following. For each decision tree; a sample of points represented in its geometric features are trained into that tree to find the different relations between points' features and corresponding outputs. This process is repeated for other decision trees used. The process of classifying any unknown point is to implement that point in each decision tree to reach a class of that tree. A voting step is then applied between the results of all trees to classify that point to the most occurrence class among the trees.

2.4.2. Gaussian Naïve Bayes

Naïve Bayes classifiers are simple probabilistic classifiers. They are based on the Bayes' theorem but with strong independence assumptions inside the features. GNB is a variant of Naïve Bayes that follows Gaussian normal distribution and supports continuous data. (Bishop, 2006). The main steps of GNB are calculating the probability of each class which equals to the portion of class' points in the whole dataset, and constructing a Gaussian distribution of each class for each feature. To classify any unknown point, a value is calculated of the point for each class according to Equation (3), and the point is classified to the class of highest value.

$$\log P(class_i) + \sum_{j \in F} \log L\left(feature_j | class_i\right) \quad (3)$$

Where $P(class_i)$ is the probability of each class, and $L\left(feature_j | class_i\right)$ is the likelihood of each $feature_j$ of $class_i$, and F is the number of features.

2.4.3. Quadratic Discriminate Analysis

A quadratic classifier is a statistical classifier that uses a quadratic decision surface to separate measurements of two or more classes of objects or events (Bishop, 2006). The algorithm represents the points according to their attributes (features) on multi-dimensional graph. Then, it builds a quadratic boundary between classes that enclose each class entire a single boundary. To classify any point, it is located on the graph according to its features and is classified to the class boundary it is inside.

3. Study Area and Dataset

To evaluate the proposed methodology, we used a pre-labelled benchmark dataset (Paris Lille 3D). It is a part of NPM3D Benchmark Suite research project (Roynard et al., 2018). It was acquired using a MLS system of robotics center of Mines Paris Tech (L3D2). The dataset consists of two parts; a longitudinal section of about 1500 m length with about 98 million points in Lille and another part in Paris with 450 length and about 45 million points.

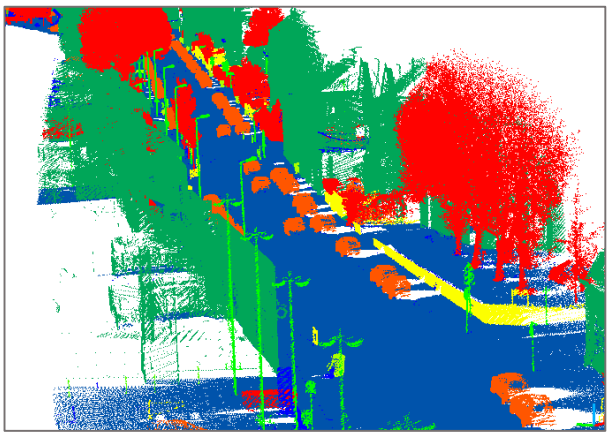

Figure 6. Paris-Lille-3D dataset (Lille Part)

The dataset contains mainly nine coarse classes in addition to some unclassified points, the classes are ground, building, pole, bollard, trashcan, barrier, pedestrian, car and vegetation. Figure 7 shows the data portion of different classes, some classes (both ground and building represent about 90% of the dataset)

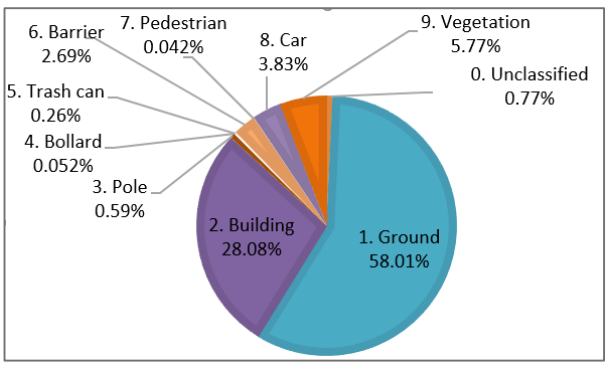

Figure 7. Dataset portion of classes

4. RESULTS

This research aimed at the comparison between three ML classifiers with three different neighborhood methods. According to (Zheng et al., 2017, 2018) ,the change and the increase in the radius of the cylinder did not have a remarkable effect, hence we used the radius of the cylinder to equal 0.20m, and similarly we choose the sphere radius to be 0.20m. For the kNN method, we chose k = 10, as in the research of (Weinmann et al., 2015), the most occurrence value as an optimal value. For each point in the dataset, its neighbors were defined and the geometric features, were derived as presented in Table 1.

The dataset was divided into two equal parts after replacing the coordinates of each point with their corresponding extracted geometric features. The two parts are training/validation part as well as the testing part. The first part was divided into four partitions, from which four ML models were created to find out the best fitting model according to the overall accuracy, after that our method could be evaluated with the remaining testing part. This procedure was implemented in all our classification scenarios whether the change in the classifier or the neighbourhood search method.

Overall accuracy was used as a primary score for the models as shown in Figure 8. In the three neighborhood methods, cylindrical neighborhood was the best between the three neighborhood methods, regardless the ML classifier used. The overall accuracy of the cylindrical method for the RF, GNB and QDA was 92.39%, 78.47% and 78.18%, respectively. On the other hand, a great difference does exist between RF and other classifiers which makes RF is the most suitable classifier for the tested dataset.

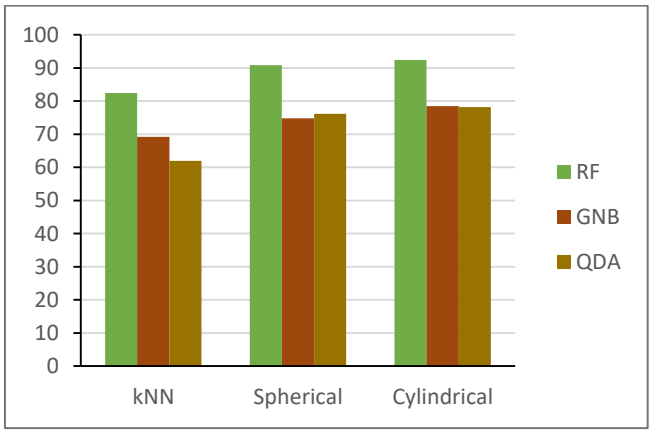

Figure 8. Overall accuracy percent of RF, GNB, and QDA for KNN, spherical, and cylindrical neighborhood.

Other scores, including precision, recall and f1-score were used to individually evaluate the results of each class. Mobile LiDAR point clouds data of road environments are usually imbalanced, and two or three classes may consist more than 90% of the whole dataset. Consequently, any ML model may be confused and tend to classify most of the points to the major class(s). As shown in Figure 7, the ground and building classes contain about 90% of the dataset, whereas the ML classifier could classify the whole points to one of these two classes, and hence the overall accuracy could reach

up to 90% but with misleading classification. Therefore, the role of using precision, recall and f1-score is to evaluate the classifiers with datasets that have low percentages of classes.

Figure 9 shows the calculated precision, recall and f1 score of each class using to different classifiers and neighborhood search methods. The ground and building classes achieved high results in the three classifiers. This comes from the large amount of points in the dataset of both classes. Therefore, any classifier will easily detect classes with large portions such as ground and building, and hence they could not be a measure for a good classifier. For instance, the precision of ground class was 98.11%, 96.66% and 97.68%, while the recall was 91.35%, 88.1% and 87.95% and f1-score was 94.61%, 92.18 and 92.56% for RF, GNB and QDA, respectively. For building class, the precision was 95.60%, 76.27% and 81.21%, while the recall was 92.65%, 90.25% and 87.14% and f1-score was 94.1%, 82.67 and 84.07% for RF, GNB and QDA, respectively.

On the other hand, the other classes are varying in their classification results, between the three classifiers; the RF revealed the highest scores between the three classifiers for detecting those low portion classes. Generally, the results showed that RF is much more effective than other classifiers. RF is also suitable to classes with less number of points such as poles, barriers, and trashcans. Therefore, classes with variant geometric characteristics require large scale of features to best distinguish between them. However, not all classifiers are able to handle all classes with a huge number of samples as well as many features. GNB and QDA classifiers were not able to achieve high scores for all classes. Only ground and building classes revealed close results for different classifiers. Ground and building were clearly distinguished due to their geometric shapes (i.e., 2D planes) which were determined using Verticality feature. Thus, this is helpful for any classifier to best find most of points that belong to those classes.

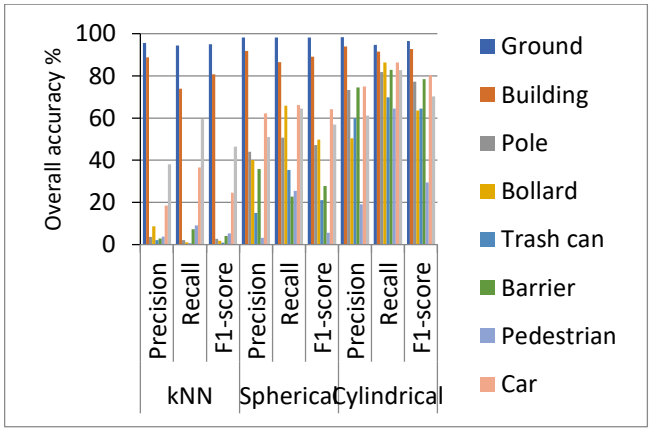

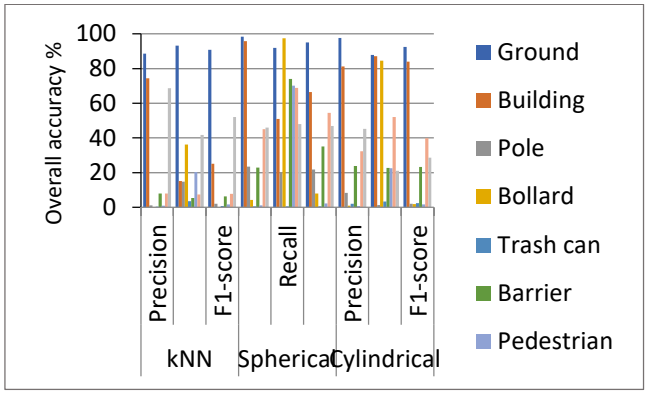

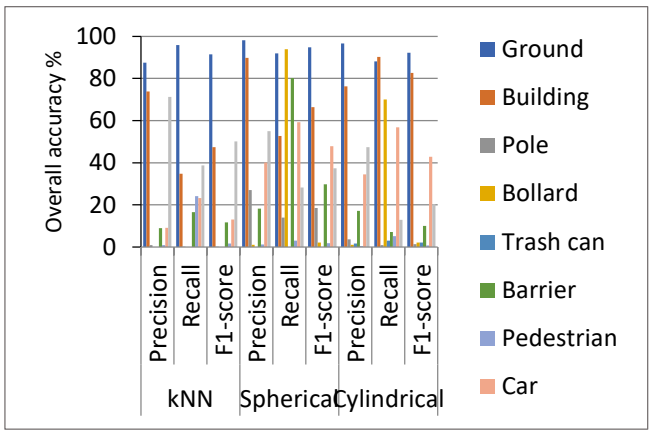

Figure 9. Classification results of RF, GNB, and QDA.

The classes could represent an obstacle and mislead the classification process. It may be a class which misleads the algorithm for the purpose of finding other classes. For example in Figure 10, the white points were wrongly classified due to the similar geometric properties with other classes.

Bottom base of vegetation (class 9 in our dataset) is an example, as nearly all bottom bases were classified wrongly. The similarity between points in different classes makes it not trivial task to classify those points. Literality, points on tree base are very similar to ground and curb points. They all have the same orientation and nearly the same height but different classes, and that make it difficult for any classifier.

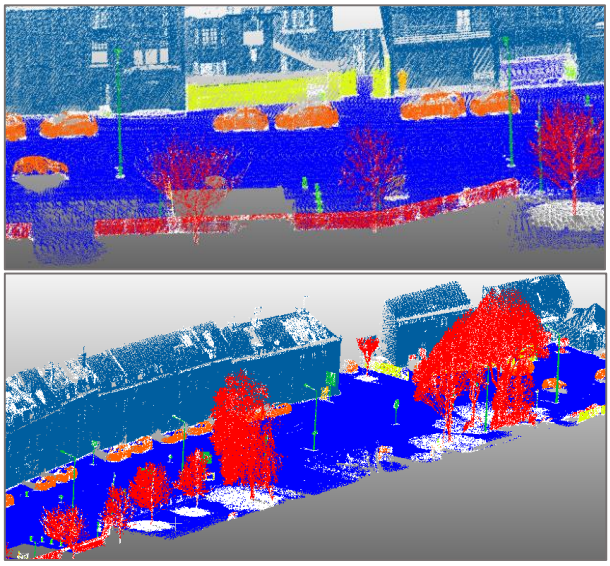

Figure 10. Example of wrongly classified points

5. CONCLUSION

Nowadays, the growth in the utilization of mobile LiDAR scanning systems is very rapid in many road corridors' applications. They have an advantage of there is no required direct contact with any road features in the data acquisition. That makes the MLS systems preferable for applications such as infrastructure and surveying assets. They capture huge amount of point clouds which describe road scenes with high details. The detection of different road features such as light poles, curb, and road signs from MLS point cloud is important to be automatic. The extracted information could be used in various applications such as quantity and volume surveys, right-of-way asset inventory and GIS applications.

In this research, three neighborhood search methods were studied and compared, namely KNN, spherical and cylindrical neighborhoods. Their results were varying and have revealed that cylindrical neighborhood method was the most suitable for the tested dataset. Although the overall accuracy of both the spherical and cylindrical was close using different classifiers with imbalanced dataset, the overall accuracy could not be a final judgment. However, and according to precision, recall and f1-score, the cylindrical neighborhood method was much more effective than the spherical one.

ML classifiers are various and differ in their mathematical models. According to the case study and type of dataset, the appropriate classifier could be selected. Three ML were applied for road features' classification from mobile LIDAR dataset to evaluate which classifier is more suitable. Three models were trained on the dataset using the three classifiers and their overall accuracy were 92.39%, 78.47% and 78.18% for RF, GNB and QDA, respectively with cylindrical neighborhood method. From the overall accuracy and the detailed scores (precision, recall and f1-score), the RF was the most suitable for the classification process. In addition, RF achieved high scores for each class including classes with low portion while those classes may be considered non-existent for the other two classifiers due to their very low scores.

Acknowledgement

The authors would like to thank the editor and the anonymous reviewers for their valuable comments and suggestions, which helped to improve this work.

Author contributions

Mahmoud Mohamed: Methodology, Software, Data curation, Validation, Visualization, Writing-Original draft preparation. **Salem Morsy:** Conceptualization, Methodology, Visualization, Writing-Reviewing and Editing. **Adel El-Shazly:** Conceptualization, Writing-Reviewing and Editing.

Conflicts of interest

There is no conflict of interest between the authors.

Statement of Research and Publication Ethics

The authors declare that this study complies with Research and Publication Ethics.

REFERENCES

Bishop, C. M. (2006). Pattern recognition. Machine Learning, 128(9).

Blomley, R., Jutzi, B., & Weinmann, M. (2016). 3D semantic labeling of ALS point clouds by exploiting multi-scale, multi-type neighborhoods for feature extraction.

Bonaccorso, G. (2017). Machine learning algorithms. Packt Publishing Ltd.

Breiman, L. (2001). Random forests. Machine Learning, 45(1), 5–32.

Burkov, A. (2019). The hundred-page machine learning book (Vol. 1). Andriy Burkov Canada.

Chehata, N., Guo, L., & Mallet, C. (2009). Airborne lidar feature selection for urban classification using random forests.

Demantké, J., Mallet, C., David, N., & Vallet, B. (2011). Dimensionality based scale selection in 3D lidar point clouds.

Dittrich, A., Weinmann, M., & Hinz, S. (2017). Analytical and numerical investigations on the accuracy and robustness of geometric features extracted from 3D point cloud data. ISPRS Journal of Photogrammetry and Remote Sensing, 126, 195–208.

Filin, S., & Pfeifer, N. (2005). Neighborhood systems for airborne laser data. Photogrammetric Engineering & Remote Sensing, 71(6), 743–755.

Guarnieria, A., Vettorea, A., Pirottia, F., & Maranib, M. (2009). Filtering of TLS point clouds for the generation of DTM in salt-marsh areas. Laser Scanning, 1–2.

Hackel, T., Wegner, J. D., & Schindler, K. (2016). Fast Semantic Segmentation of 3D Point Clouds With Strongly Varying Density. ISPRS Annals of Photogrammetry, Remote Sensing and Spatial Information Sciences, III–3(July), 177–184. https://doi.org/10.5194/isprsannals-iii-3-177-2016

Hyyppä, J., Jaakkola, A., Chen, Y., & Kukko, A. (2013). Unconventional LIDAR mapping from air, terrestrial and mobile. Proceedings of the Photogrammetric Week, 205–214.

Lee, I., & Schenk, T. (2002). Perceptual organization of 3D surface points. International Archives of Photogrammetry Remote Sensing and Spatial Information Sciences, 34(3/A), 193–198.

Linsen, L., & Prautzsch, H. (2001). Local versus global triangulations. Proceedings of EUROGRAPHICS, 1, 257–263.

Li, Q., Yuan, P., Lin, Y., Tong, Y., & Liu, X. (2021). Pointwise classification of mobile laser scanning point clouds of urban scenes using raw data. Journal of Applied Remote Sensing, 15(2), 24523.

Mallet, C., Bretar, F., Roux, M., Soergel, U., & Heipke, C. (2011). Relevance assessment of full-waveform lidar data for urban area classification. ISPRS Journal of Photogrammetry and Remote Sensing, 66(6), S71–S84.

Mohamed, M., Morsy, S., & El-Shazly, A. (2021a). Evaluation of data subsampling and neighbourhood selection for mobile LiDAR data classification. The Egyptian Journal of Remote Sensing and Space Science, 24(3), 799–804.

Mohamed, M., Morsy, S., & El-Shazly, A. (2021b). Machine Learning for Mobile LIDAR Data Classification of 3d Road Environment. ISPRS-International Archives of the Photogrammetry, Remote Sensing and Spatial Information Sciences, 44, 113–117.

Nguyen, V.-T., Constant, T., Kerautret, B., Debled-Rennesson, I., & Colin, F. (2020). A machine-learning approach for classifying defects on tree trunks using terrestrial LiDAR. Computers and Electronics in Agriculture, 171, 105332.

Pauly, M., Keiser, R., & Gross, M. (2003). Multi-scale feature extraction on point-sampled surfaces. Computer Graphics Forum, 22(3), 281–289.

Pu, S., & Vosselman, G. (2009). Knowledge based reconstruction of building models from terrestrial laser scanning data. ISPRS Journal of Photogrammetry and Remote Sensing, 64(6), 575–584.

Roynard, X., Deschaud, J. E., & Goulette, F. (2018). Paris-Lille-3D: A large and high-quality ground-truth urban point cloud dataset for automatic segmentation and classification. International Journal of Robotics Research, 37(6), 545–557. https://doi.org/10.1177/0278364918767506

Wang, Y., Jiang, T., Yu, M., Tao, S., Sun, J., & Liu, S. (2020). Semantic-based building extraction from LiDAR point clouds using contexts and optimization in complex environment. Sensors, 20(12), 3386.

Weinmann, M., Jutzi, B., Hinz, S., & Mallet, C. (2015). Semantic point cloud interpretation based on optimal neighborhoods, relevant features and efficient classifiers. ISPRS Journal of Photogrammetry and Remote Sensing, 105, 286–304. https://doi.org/10.1016/j.isprsjprs.2015.01.016

Weinmann, M., Jutzi, B., & Mallet, C. (2013). Feature relevance assessment for the semantic interpretation of 3D point cloud data. ISPRS Annals of the Photogrammetry, Remote Sensing and Spatial Information Sciences, 2(5W2), 313–318. https://doi.org/10.5194/isprsannals-II-5-W2-313-2013

Weinmann, M., Jutzi, B., & Mallet, C. (2014). Semantic 3D scene interpretation: A framework combining optimal neighborhood size selection with relevant features. ISPRS Annals of Photogrammetry, Remote Sensing and Spatial Information Sciences, II–3(September), 181–188. https://doi.org/10.5194/isprsannals-ii-3-181-2014

Weinmann, M., Jutzi, B., Mallet, C., & Weinmann, M. (2017). GEOMETRIC FEATURES and THEIR RELEVANCE for 3D POINT CLOUD CLASSIFICATION. ISPRS Annals of the Photogrammetry, Remote Sensing and Spatial Information Sciences, 4(1W1), 157–164. https://doi.org/10.5194/isprs-annals-IV-1-W1-157-2017

Weinmann, M., Urban, S., Hinz, S., Jutzi, B., & Mallet, C. (2015). Distinctive 2D and 3D features for automated large-scale scene analysis in urban areas. Computers and Graphics (Pergamon), 49, 47–57. https://doi.org/10.1016/j.cag.2015.01.006

West, K. F., Webb, B. N., Lersch, J. R., Pothier, S., Triscari, J. M., & Iverson, A. E. (2004). Context-driven automated target detection in 3D data. Automatic Target Recognition XIV, 5426, 133–143.

Yu, Y., Li, J., Guan, H., Wang, C., & Yu, J. (2014). Semiautomated extraction of street light poles from mobile LiDAR point-clouds. IEEE Transactions on Geoscience and Remote Sensing, 53(3), 1374–1386.

Zheng, M., Lemmens, M., & van Oosterom, P. (2017). CLASSIFICATION OF MOBILE LASER SCANNING POINT CLOUDS FROM HEIGHT FEATURES. International Archives of the Photogrammetry, Remote Sensing & Spatial Information Sciences, 42.

Zheng, M., Lemmens, M., & van Oosterom, P. (2018). Classification of mobile laser scanning point clouds of urban scenes exploiting cylindrical neighbourhoods. Int. Arch. Photogramm. Remote Sens. Spat. Inf. Sci, 42, 1225–1228.

© Author(s) 2022.
This work is distributed under https://creativecommons.org/licenses/by-sa/4.0/

Advanced LiDAR
http://publish.mersin.edu.tr/index.php/lidar/index
e-ISSN 2791-8572

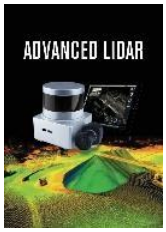

Availability of Iphone 13 Pro Laser Data in 3D Modeling

İlyas Aslan[1], Nizar Polat[*2]

[1]*Dicle University, Vocational School of Technical Sciences, Architecture and Urban Planning, Diyarbakır, Turkey*
[2]*Harran University, Faculty of Engineering, Survey Engineering, Şanlıurfa, Turkey*

Keywords
Lidar,
Photogrammetry,
İphone 13 Pro,
Diyarbakır.

ABSTRACT

Today, photography and, accordingly, photogrammetry approach are used extensively in the documentation of cultural assets and the creation of three-dimensional models. Many advantages such as speed, accuracy and digital processing provided by photogrammetry have been effective in this widespread use. With the developing technologies, the reduction of sensor sizes has opened new doors in digital data production. As of 2020, it has been possible to integrate laser scanning sensors into mobile devices. For the first time, with the iPad Pro and iPhone 12 Pro devices, Apple started to use the built-in LiDAR sensors in its non-professional devices as well as the digital camera. This situation has opened up new opportunities in the documentation of cultural heritage. In this study, three-dimensional models of the historical Aslanlı fountain in İçkale of the Centre Sur district of Diyarbakır province were produced using both photograph and laser data of iPhone 13 Pro and the results of the two data were compared.

1. INTRODUCTION

The preservation and promotion of cultural heritage is becoming more and more popular day by day. For this, promotion is very important. Cultural Heritage makes the city effective in terms of social and representation of the city's identity. When documentation, presentation and communication are used effectively, the city can be promoted correctly. (Korunmaz vd. 2011; Oruç, 2021; Yakar ve Yılmaz, 2008; Alptekin and Yakar., 2020; Alptekin et al., 2019a).

Metric, written and visual documentation provides benefits in determining the problems of cultural heritage and transferring this heritage to future generations. Today, documentation studies have become very rich in terms of method diversity together with technology. In this respect, making the cultural heritage permanent with documentation methods ensures that the city develops and makes it important socially, culturally and economically. (Yakar vd., 2005; Uslu vd., 2016; Yaman & Kurt 2019; Alptekin et al., 2019b; Altuntas et al., 2007; Ulvi and Yakar, 2014).

Recently, many attempts have been reported regarding 3D documentation and modeling of small artifacts using various methods or approaches. The basic feature of digitizing a work as a small object may vary depending on its size. (Yakar vd., 2009; 2010).

Photogrammetry provides significant opportunities for three-dimensional location information, spatial analysis, simulations and visualization for cultural heritage.

3D models created with the photogrammetry method are formed in real size and appearance. Photogrammetric measurement systems allow the real object geometry to be determined as well as modeling the object with its georeference. In addition, these

[*]Corresponding Author
*(ilyas.aslan@dicle.edu.tr) ORCID ID 0000-0003-4388-6633
(nizarpolat@harran.edu.tr) ORCID ID 0000-0002-6061-7796

Cite this;
Aslan, İ. & Polat, N. (2022). Availability of Iphone 13 Pro Laser Data in 3D Modeling. Advanced LiDAR, X(X), 10-14.

technologies allow 3D models with real images, especially since they are processed with the real image of the object (Ulvi vd. 2020; Şenol & Kaya 2019; Yılmaz and Yakar., 2006a; Yılmaz and Yakar., 2006b).

Lidar (Light Detection and Ranging) technology has been used in various fields since it entered our lives. It is used for 3D modeling of structures, restoration, natural disasters, coastal protection, forest management and determining the amount of deformation in bridges. (Alptekin vd. 2019b).

With the laser scanner, millions of points are shot at the object within minutes, and the points that hit the object and return are recorded. There are three types of laser scanners: air, terrestrial and mobile. (Alptekin, Yakar, 2020; Ulvi et al., 2014; Yakar et al., 2009; Yakar et al., 2014)

As a data collection tool, laser scanning devices integrated into mobile phones and tablets have been used in recent years.

In this study, the Aslanli fountain was scanned using the iPhone 13 pro lidar sensor.

2. WORKING AREA

The historical Aslanlı fountain at the entrance of the inner castle, located in the central Sur district of Diyarbakır, was chosen as the application area. 19th century The Aslanlı fountain, dated to the end of the B.C., was built from neatly cut basalt stone. The fountain is enclosed in a low arched niche. At the top, there is a triangular pediment that draws attention on two white short columns, and the fountain is crowned with this pediment. Water flows from the mouth of the lion, which was originally placed in a niche with a three-slice arch. (URL-1)

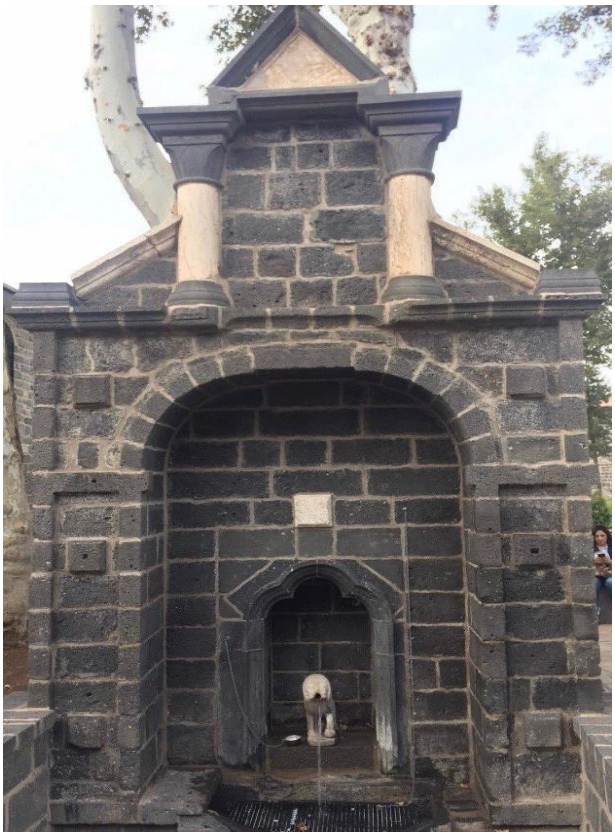

Figure 1. Aslanlı fountain(URL-2)

3. METHOD

In the application, both Photogrammetry and Lidar studies were carried out.

Lidar application was realized with Iphone 13 pro laser sensor. The photogrammetry application was taken with the same device, the iPhone 13 pro camera.

3.1. Lidar Sensor

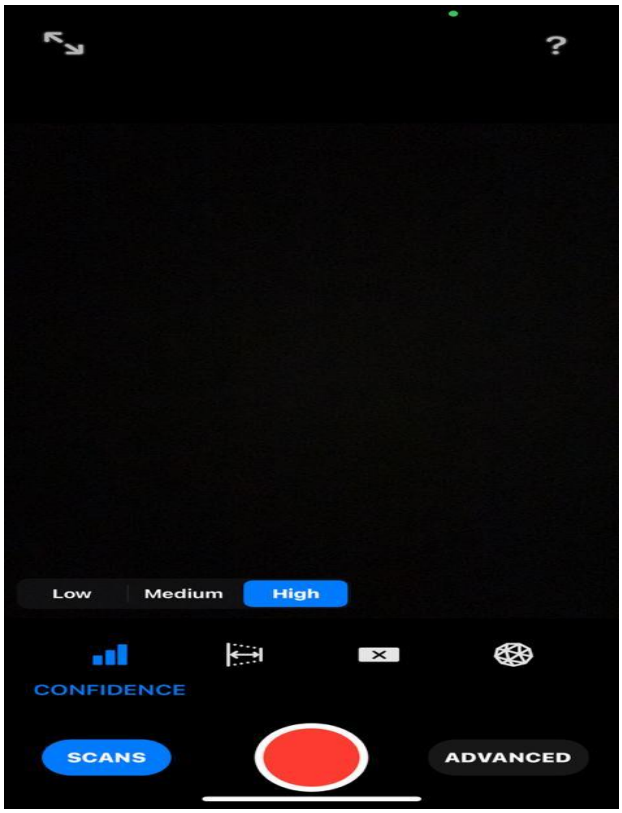

Figure 2. Product quality in lidar measurement

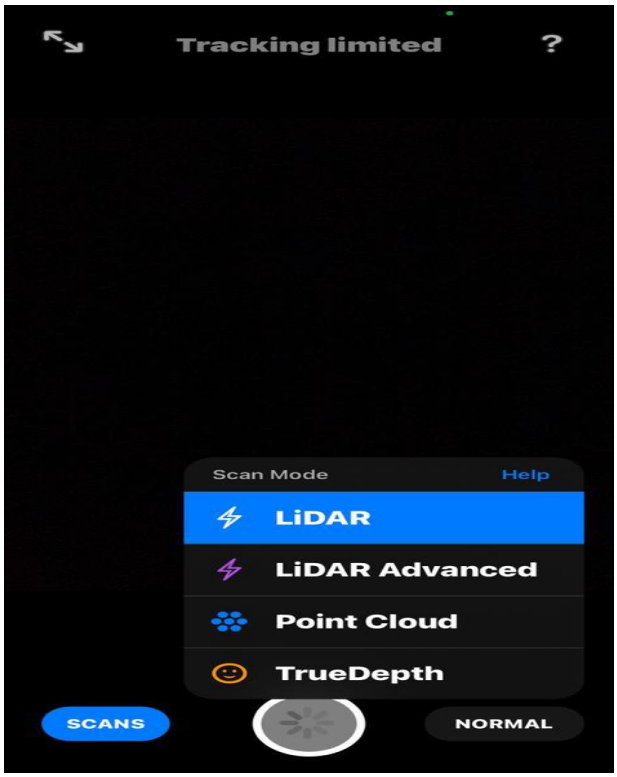

Figure 3. Four different lidar measurement methods

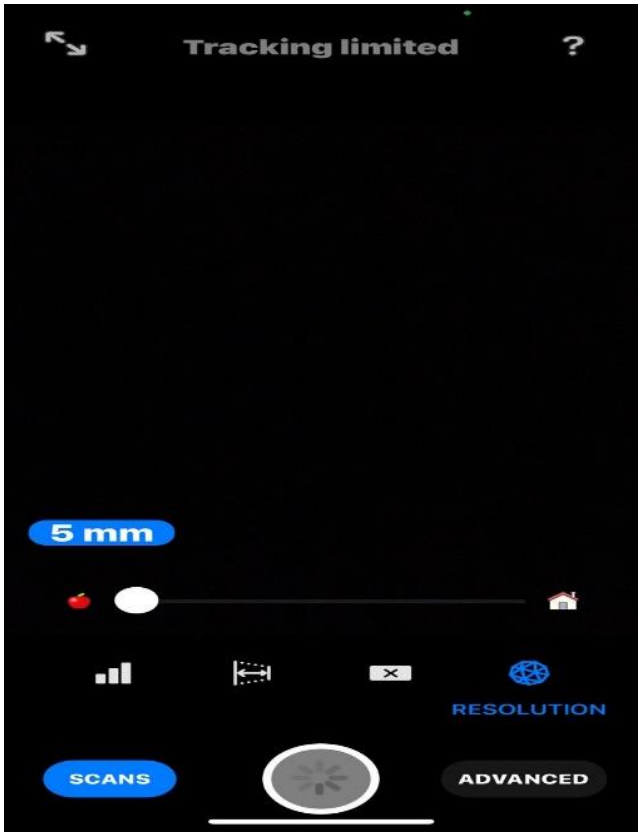

Figure 4. Cloud spacing for smallest object

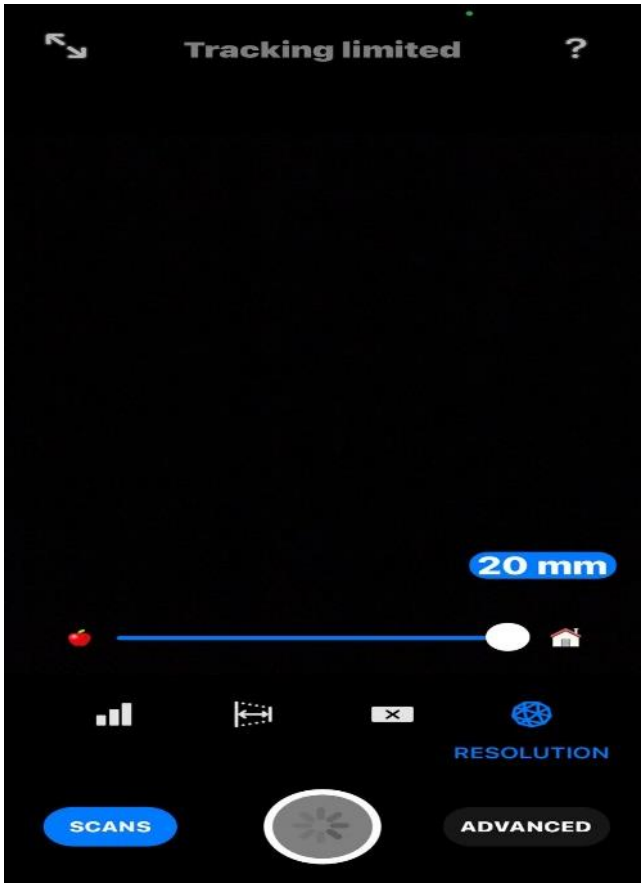

Figure 6. Cloud spacing for largest object

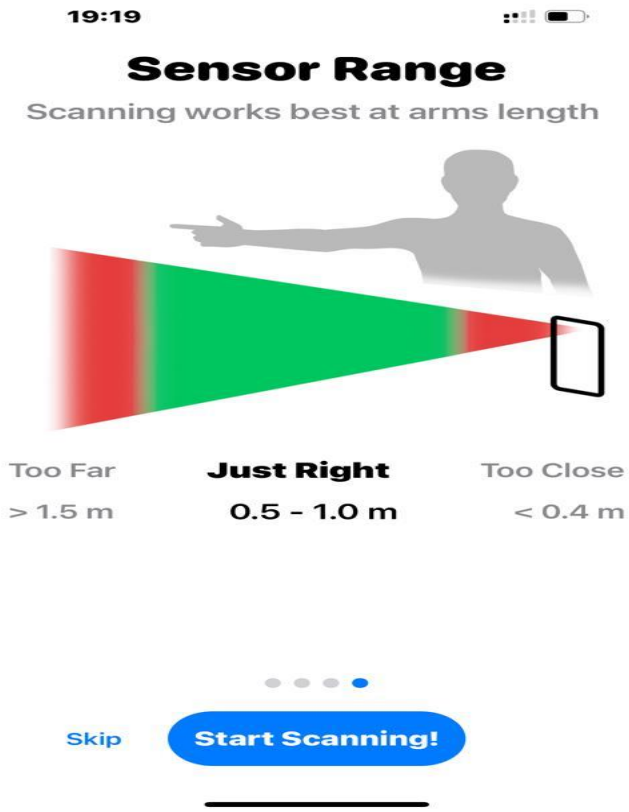

Figure 7. Top quality lidar scan distance range

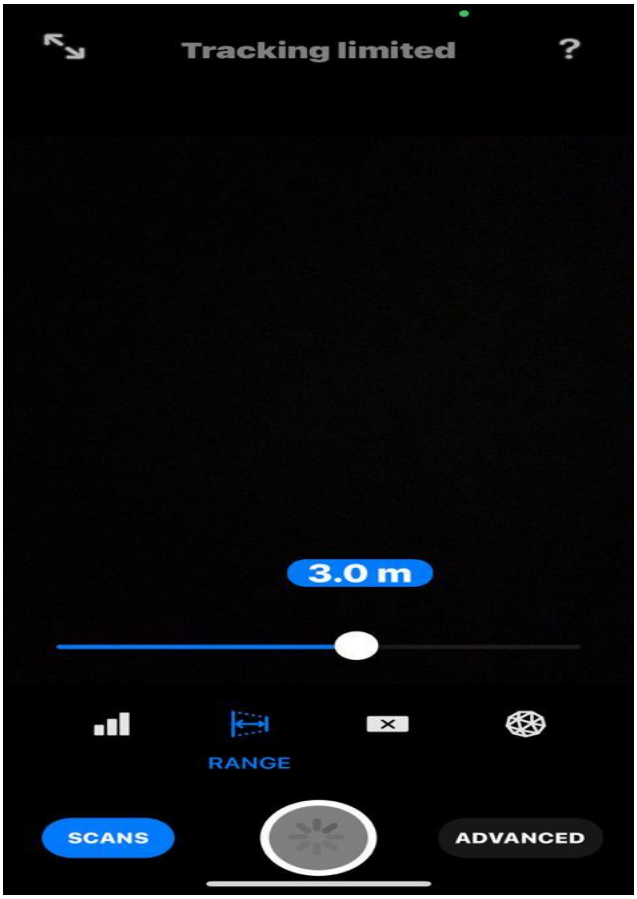

Figure 8. Object scanning distance range 1m-5m

3.2. Camera Sensor

The camera features on the iPhone 13 pro are as follows:
-12 MP Pro camera system: Telephoto, Wide and Ultra Wide cameras
-3x optical zoom, 2x optical zoom; 6x optical zoom range
-Up to 15x digital zoom
-Portrait shooting in Night mode with the help of LiDAR Scanner
-Portrait mode with advanced bokeh effect and Depth Control
-Portrait Lighting with six effects (Natural, Studio, Contour, Stage, Stage Mono, High-Key Mono)
-Sensor-based optical image stabilization (Wide)
-Six-element lens (Telephoto and Ultra Wide); seven-element lens (Wide)
-True Tone Flash with Slow Sync
Panorama (up to 63 MP) (URL-3)

4. RESULTS

4.1. Photogrammetric analyzes

-Photogrammetric point cloud 4128860 points.
-Photogrammetric point cloud is denser (average 320 nkt/m2)
-There is no access to the battlement in front of the fountain.
-Data collection and processing takes longer.
(no device heating and battery restrictions)
-There are too many unnecessary points in the areas outside the object.
-Object integrity is broken in areas that cannot be photographed.

Figure 9. Photogrammetric point cloud

4.2. Lidar application analysis

-Point cloud with iphone 13 lidar, 504126 points.
-Less dense than photogrammetric point cloud (average 40 nkt/m2)
-Laser beams reach into the loophole in front of the fountain
-Data collection and processing is shorter.
(there are device heating and battery limitations)
-Less due to unnecessary point orientation in non-object areas.
-Object integrity is broken in areas that cannot be scanned.

Figure 10. Point cloud with lidar

As seen in the figure below, the point cloud distance between the two applications is 11 cm.

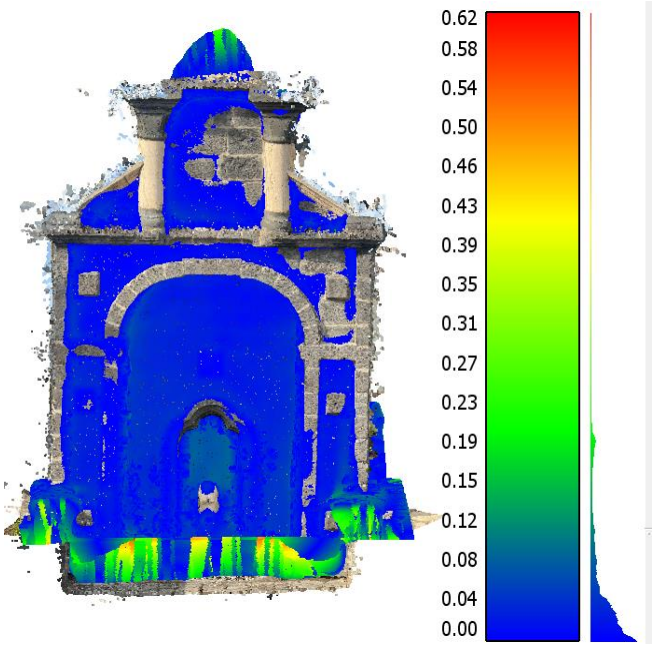

Figure 11. The average distance between two point clouds is 11 cm.

5. CONCLUSION

-The iPhone 13 lidar sensor can be used to collect data on short-term outdoor objects.
-Repeat scanning is possible to increase data density.
-It can be used integrated with the photogrammetric point cloud.
-It can be used in 3D models due to the built-in camera integration.

Author contributions

The authors contributed equally.

Conflicts of interest

There is no conflict of interest between the authors.

Statement of Research and Publication Ethics

The authors declare that this study complies with Research and Publication Ethics

References

Alptekin, A. & Yakar, M. (2020). Mersin Akyar Falezi'nin 3B modeli. Türkiye Lidar Dergisi, 2(1), 5-9.

Alptekin, A., Çelik, M. Ö. & Yakar, M. (2019a). Anıtmezarın yersel lazer tarayıcı kullanarak 3B modellenmesi. Türkiye Lidar Dergisi, 1(1), 1-4.

Alptekin, A., Fidan, Ş., Karabacak, A., Çelik, M. Ö. & Yakar, M. (2019b). Üçayak Örenyeri'nin yersel lazer tarayıcı kullanılarak modellenmesi. Türkiye Lidar Dergisi, 1(1), 16-20.

Altuntas, C., Yildiz, F., Karabork, H., Yakar, M. & Karasaka, L. (2007, October). Surveying and documentation of detailed historical heritage by laser scanning. In XXI International CIPA Symposium (Vol. 1, No. 06).

Korumaz, G, A., Dülgerler, O. N. & Yakar, M. (2011). Kültürel mirasın belgelenmesinde dijital yaklaşımlar. Selçuk Üniversitesi Mühendislik Mimarlık Fakültesi Dergisi, 26 (3), 63-86.

Şenol, H. İ. & Kaya, Y. (2019). İnternet Tabanlı Veri Kullanımıyla Yerleşim Alanlarının Modellenmesi: Çiftlikköy Kampüsü Örneği. Türkiye Fotogrametri Dergisi, 1(1), 11-16

Ulvi, A. & Yakar, M. (2014). Yersel Lazer Tarama Tekniği Kullanarak Kızkalesi'nin Nokta Bulutunun Elde Edilmesi ve Lazer Tarama Noktalarının Hassasiyet Araştırması. Harita Teknolojileri Elektronik Dergisi, 6(1), 25-36.

Ulvi, A., Yakar, M., Toprak, A. S., & Mutluoglu, O. (2014). Laser Scanning and Photogrammetric Evaluation of Uzuncaburç Monumental Entrance. International Journal of Applied Mathematics Electronics and Computers, 3(1), 32-36.

Ulvi, A., Yakar, M., Yiğit, A. Y. & Kaya, Y. (2020). İHA ve yersel fotogrametrik teknikler kullanarak Aksaray Kızıl Kilise'nin 3 boyutlu nokta bulutu ve modelinin üretilmesi, Geomatik Dergisi, 5, 1, 22-30.

Yakar, M. & Yılmaz, H. M. (2008). Kültürel Miraslardan Tarihi Horozluhan'ın Fotogrametrik Rölöve Çalışması Ve 3 Boyutlu Modellenmesi. Selçuk Üniversitesi Mühendislik, Bilim Ve Teknoloji Dergisi, 23(2), 25-33.

Yakar, M., Yıldız, F., & Yılmaz, H. M. (2005). Tarihi Ve Kültürel Miraslarin Belgelenmesinde Jeodezi Fotogrametri Mühendislerinin Rolü. TMMOB Harita ve Kadastro Mühendisleri Odası, 10

Yakar, M., Yılmaz, H. M. & Mutluoğlu, H. M. (2009). Hacim Hesaplamalarında Laser Tarama ve Yersel Fotogrametrinin Kullanılması, TMMOB Harita ve Kadastro Mühendisleri Odası 12. Türkiye Harita Bilimsel ve Teknik Kurultayı, Ankara.

Yakar, M., Yilmaz, H. M. & Mutluoglu, O. (2014). Performance of Photogrammetric and Terrestrial Laser Scanning Methods in Volume Computing of Excavtion and Filling Areas. Arabian Journal for Science and Engineering, 39(1), 387-394.

Yaman, A. & Kurt, M. (2019). Investigation of the possibilities of using Geoslam terrestrial laser scanner for documentation and three-dimensional modeling of historical and cultural heritage: Example of Ulucami in Aksaray Province, Türkiye Lidar Dergisi 1(1), 5-9.

Yılmaz, H. M. & Yakar, M. (2006a). Lidar (Light Detection And Ranging) Tarama Sistemi. Yapı Teknolojileri Elektronik Dergisi, 2(2), 23-33.

Yılmaz, H. M. & Yakar, M. (2006b). Yersel lazer tarama Teknolojisi. Yapı teknolojileri Elektronik dergisi, 2(2), 43-48.

URL-1 http://www.diyarbakirkulturturizm.org/Yapit/Details/IC-KALE/20/Aslanli-Cesme/195

URL-2 https://www.gastrodiyar.com/tarihi yerler/kategori/ic-kale

URL-3 https://www.apple.com/tr/iphone-13-pro/specs/.

© Author(s) 2022.
This work is distributed under https://creativecommons.org/licenses/by-sa/4.0/

Advanced LiDAR

http://publish.mersin.edu.tr/index.php/lidar/index

e-ISSN 2791-8572

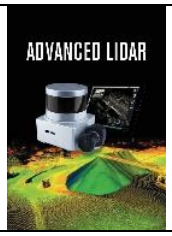

The Feature Extraction from Point Clouds using Geometric Features and RANSAC Algorithm

Ramazan Alper Kuçak[*1]

[1]*Niğde Ömer Halisdemir University, Faculty of Engineering, Department of Geomatics, Turkey*

Keywords
LiDAR
TLS
Point Cloud
RANSAC
3D Model

ABSTRACT

The feature extraction of point clouds is essential for geomatics engineering as well as other engineering and architectural applications. Furthermore, with the recent entrance of digital twins, virtual reality, 3D city modeling, reverse engineering, and metaverse into human existence, 3D models, which are currently used in numerous technical sectors, have become increasingly important. As a result, the 3D model generating methods become more important. One of the most prevalent methodologies used by scientists is range-based modeling (e.g., laser scanning). Additionally, before being visualized or analyzed for 3D surfaces, 3D model acquisition (Light Detection and Ranging (LiDAR) or structure-from-motion (SfM)) and 2D imaging approaches are commonly converted into models such as 3D mesh and parameter surface. This study analyzed 3D point cloud data obtained with terrestrial laser scanners. Also, many approaches to model extraction have been tried to obtain 3D models, planes, corner points, and lines by using various 3D surface analyses and Random Sample Consensus (RANSAC) Algorithm.

1. INTRODUCTION

With the recent entrance of technologies such as digital twins, virtual reality, 3D city modeling, reverse engineering, and metaverse into human existence, 3D models, which are currently employed for cultural heritage or diverse engineering sectors, have grown in importance. From the past to the present, historical artifacts have been subjected to a variety of natural and artificial destructions. Because research into preserving cultural assets for enlightening future generations about history is accelerating around the world, and its (3D Models) relevance is overgrowing. (Kuçak, R. A., 2013; Kuçak, R. A., et al., 2016; Alptekin and Yakar., 2020; Alptekin et al., 2019a; Alptekin et al., 2019b)

Nowadays, non-contact approaches based on light waves, notably active or passive sensors, are used to produce 3d models for cultural heritage or archaeological sites. For object and scene modeling, there are now four options:

1. Image-based rendering, which does not build the geometry of a 3D model but could be used to construct virtual aspects.
2. Image-based modeling (e.g., photogrammetry), the preferred method for preserving architectural structures' geometric surfaces and cultural heritage.
3. Range-based modeling (e.g., laser scanning) is becoming a typical approach for scientists and non-expert users such as Cultural Heritage personnel.
4. The combination of image and range-based modeling, as each has advantages and weaknesses, and their integration can allow for the efficient and rapid development of detailed 3D models. (Almagro A. and Almagro Vidal A., 2007, Kuçak, R. A., et al., 2016, Korumaz, S. A. G. 2021; Altuntas et al., 2007; Ulvi and Yakar, 2014)

*Corresponding Author

*(akucak@ohu.edu.tr) ORCID ID 0000-0002-1128-1552

Cite this;

Kuçak, R. A. (2022). The Feature Extraction from Point Clouds using Geometric Features and RANSAC Algorithm. Advanced LiDAR, 2(1), 15-20.

Research Article

Accepted: 25/03/2022

Laser scanning is a modern technology that allows multiple 3D scans to be acquired in a short amount of time, whether from the air or on the ground. It creates a 3D point cloud with intensity values in a local coordinate system; internal or external digital cameras usually provide extra information such as RGB values. Laser scanners can be used on the ground or as component of an aircraft. Laser scanning, on the other hand, produces a point cloud, which is a set of XYZ coordinates in a coordinate system that depicts to the observer a knowledge of a subject's spatial distribution. Pulse, amplitude, intensity, and RGB values may also be included. (Kuçak, Kiliç, & Kisa, 2016; Ulvi et al., 2014, Yakar et al., 2009, Yakar et al., 2014))

The Random Sample Consensus (RANSAC) method (Fischer and Bolles, 1981) extracts forms by constructing candidate shape primitives by drawing minimal data points at random. If the primitives have some semantic meaning, a categorization is also performed. Then, the candidate shapes are compared to all points in the dataset to establish a value for the number of points that reflects the most excellent match. Locally fitting primitives like planes, cylinders, and cones using RANSAC-based algorithms is a popular reverse engineering strategy (Schnabel et al. 2009). (Grilli, E., et al.,2017).

Terrestrial laser scanning (TLS) data can be used by editing in various CAD programs for architectural projects. The purpose of this study is to be 3D analyze of the building scanned with 3D terrestrial laser scanning technology, after analyzed object details by scanning with the terrestrial laser scanner, the 3D models and 3D surfaces of the 3D point clouds were generated with RANSAC Algorithm. Also, the advantages and disadvantages of open source code software is to evaluate for obtaining 3D surfaces and performing various surface analysis by using an Open Source program.

In this study, the TLS point clouds are selected to model the 3D Surfaces. Thus; it is intended a contribution to the accuracy of cultural heritage 3D model and 3D city models produced with point clouds. So, the faculty of Civil Engineering located in Ayazaga Campus of ITU in Turkey was selected as study area. The study area scanned with Leica C10, which can get 50,000 points per second with 6 mm accuracy. With the RANSAC algorithm primitive shapes was extracted from the point cloud and the primitive shapes are assigned to colors that have been discovered. Also, The 3D surface analysis of 3D point cloud were carried out.

2. DATA and METHOD

The faculty of Civil Engineering located in Ayazaga Campus of ITU in Turkey was selected a study area which is an indoor data (Figure 1). The study area scanned with Leica C10, which can get 50,000 points per second with 6 mm accuracy. The study area is indoors data. The 3D surface analysis of 3D point cloud were carried out.

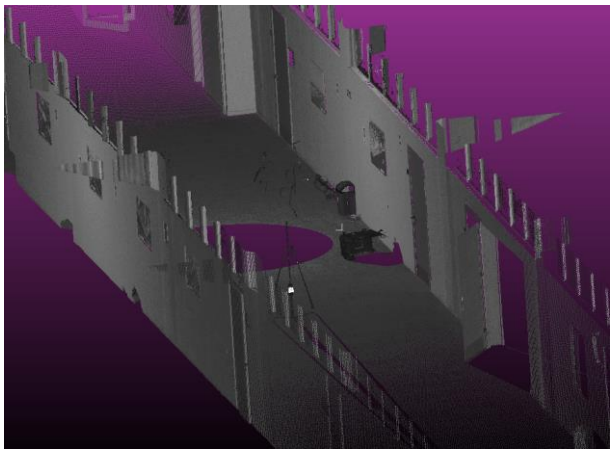

Figure 1. TLS Point Cloud indoor data (Leica C10)

2.1. Terrestrial laser scanning (TLS)

Light Detection and Ranging (LiDAR), which can be used on the ground or in the air, is an advanced technology that enables it to gather much 3D data quickly. In the local coordinate system, it generates a point cloud with intensity values; additional data, such as RGB values, are typically provided by internal or external digital cameras. (Kuçak, Kiliç, & Kisa, 2016; Kuçak, Özdemir, & Erol, 2017)

TLS is an effective technology for rapidly gathering 3D data distributed across a vast area (Kuçak et al., 2013, Kuçak et al., 2016, Kuçak et al., 2020). TLSs consist of lasers, carefully calibrated receivers, precise timing, rapid micro-controlled motors, and accurate mirrors (Fowler & Kadatskiy, 2011). The virtual point cloud generated by all of the 3D points from the surfaces that were scanned harmoniously is the fundamental data gathered from each scan (Scaioni, 2005). TLS is an effective technology for producing a 3D dense point cloud using traditional measuring techniques because of its precision and accuracy (Çelik et al., 2020). The quality of the 3D models is affected by registration errors; hence the registration of TLS scans must be done correctly.

2.2. 3D Surface Parameters

Surface parameters are used to explain the surface's local geometry. In point cloud analysis, these surface features are now routinely used. These geometric features are intended to be extracted (surfaces, lines, corners, and key points). The eigenvalues (λ_1, λ_2, λ_3) of the eigenvectors (v_1, v_2, v_3) produced from the covariance matrix of any point p of the point cloud can be used to calculate surface parameters (Table 1). (Atik, M. E., Duran, Z., & Seker, D. Z. 2021).

Table 1. Surface parameters derived from eigenvalues

Sum of eigenvalues	$\lambda_1 + \lambda_2 + \lambda_3$
Omnivariance	$(\lambda_1.\lambda_2.\lambda_3)^{\wedge}1\backslash 3$
Anisotropy	$(\lambda_1 - \lambda_3)/\lambda 1$
Planarity	$(\lambda_2 - \lambda_3)/\lambda 1$
Linearity	$(\lambda_1 - \lambda_2)/\lambda 1$
Surface variation	$\lambda_3/(\lambda_1 + \lambda_2 + \lambda_3)$
Sphericity	λ_3/λ_1
Verticality	$\lambda_1.\text{In}\ \lambda_1 + \lambda_2.\text{In}\ \lambda_2 + \lambda_3.\text{In}\ \lambda_3$
1st order moment	see Eq. (1)

Many values are calculated using eigenvalues (Table 1). (Sum of eigenvalues, omnivariance, roughness, anisotropy, planarity, linearity, surface variation, Sphericity, 1st order moments and curvatures etc.) these parameters derived from only 3D coordinates.

$$m \uparrow = \sum_{n \in P_n} (p_n - p_i).\, , v_2, \quad (1)$$

where P_n denotes the set comprising the N nearest neighbours of each individual point p_i , (.,) denotes the scalar product, v_2 is egeinvector, m ↑ is the first order moment of p_i.

Curvatures are a surface's geometrical features that are invariant according to rotation, translation, and scaling. There are many methods to calculate the Curvature of a surface. The Curvature can be calculated easily when the analytical formula is available for a surface, but these methods are not usually applicable to point clouds' surfaces. So, the surface fitting method depending on a point and its neighbors is a good way. (Foorginejad & Khalili, 2014)

For the curvature estimation, one of the most preferred methods is the covariance analysis method (Hoppe, DeRose, Duchamp, McDonald, & Stuetzle, 1992), which uses the ratio between the minimum eigenvalue and the sum of the eigenvalues. This method is known as the surface variance (Pauly, Gross, & Kobbelt, 2002). The surface variance is appropriate for point clouds because it uses the coordinate of a point and its neighbors, and it is not expensive to process. (Foorginejad & Khalili, 2014).

2.3. RANSAC Algorithm

The Random Sample Consensus (RANSAC) method (Fischer and Bolles, 1981) extracts forms by constructing candidate shape primitives by drawing minimal data points at random. If the primitives have some semantic meaning, a categorization is also performed. Then, the candidate shapes are compared to all points in the dataset to establish a value for the number of points that reflects the most excellent match. Locally fitting primitives like planes, cylinders, and cones using RANSAC-based algorithms is a popular reverse engineering strategy (Schnabel et al. 2009). (Grilli, E., et al.,2017).

The RANSAC algorithm works by searching a 3D point cloud for primitive shapes (plane, sphere, cylinder, cone, and torus). It extracts primitive shapes from point cloud data by randomly picking minimal groupings of points and fitting primitive shapes. The RANSAC algorithm computes the parameters of a basic shape by randomly drawing the least number of points (a minimum set) that may uniquely define it. The program next looks for more points in the point cloud and decides whether or not they correspond to the fitted primitive shape. The generated potential primitive forms are compared to all points in the data to see how many of them the primitive can accurately approximate. The RANSAC approach compares the recognized potential primitive shape with the last saved one in each round of iteration. If the new shape is more suitable, it will replace the old one. The best possible shape is the primitive shape that approximates the most significant number of points; its parameters were generated during the segmentation process, and the points that correspond to it can be projected onto the surface. The RANSAC algorithm extracts a primitive shape from the point cloud and continues the segmentation procedure on the remaining points. The primitive shapes that have been discovered are assigned to Colors. (Liu, J., 2020)

In the classic RANSAC formula, The starting value of t is 0, and the number of times the current iteration is calculated is t (Li, M., et al.2019).

- When t is less than the target iteration number r, data points are chosen randomly from the data collection, and a model appropriate for the data is built.
- Data points that satisfy the model are located and counted in the number of data points suitable to the model from the remaining (N num) points.
- The ideal model in this iterative process is found when the number of data points suitable to the model exceeds the stated standard number "m".
- The first step is repeated to find the best model until the iterative calculation is complete.

The probability "w" that each point taken from the point cloud data set "N" is exactly an inner point is assumed in the original RANSAC algorithm. The value of w is typically unknown; however, it can be approximated using an equation (2). (Li, M., et al.2019)

$$w = m/N \quad (2)$$

P denotes the ideal probability that the initial RANSAC method will produce a helpful model once executed. The number of iterations "r" is determined by the theoretical results (3) (Li, M., et al.2019).

$$r = In(1-P) / In(1-w^{min}) \quad (3)$$

3. RESULTS

We calculated the geometric features (Table 1) of a surface. Then, we filtered and segmented the data according to optimum values. In this way, we could quickly obtain vertices, boundary lines, and 3D surfaces from 3D point clouds.

Many values are calculated using eigenvalues (Table 1). (Sum of eigenvalues, omnivariance, roughness, anisotropy, planarity, linearity, verticality (Figure 2) surface variation, Sphericity, 1st order moment and curvatures (Figure 3) etc.) Since the datasets used contained only geometric information (3D coordinates).

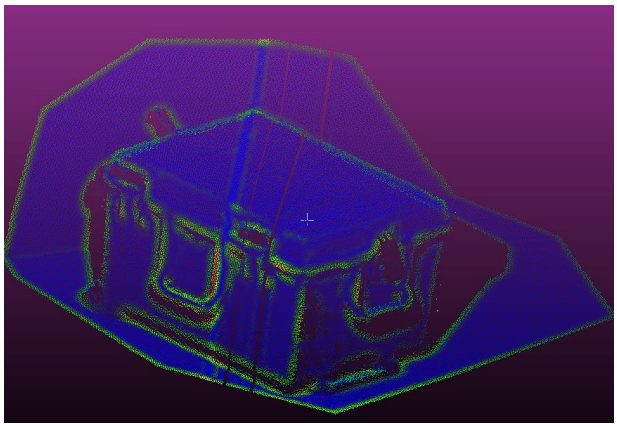

Figure 2. TLS Data According to 1st Moment (Leica C10)

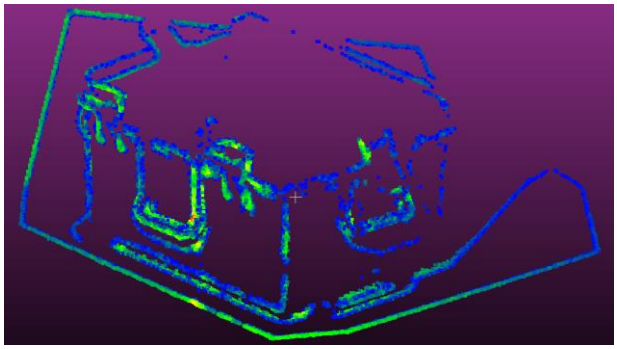

Figure 2a. Boundary lines According to 1st order Moment

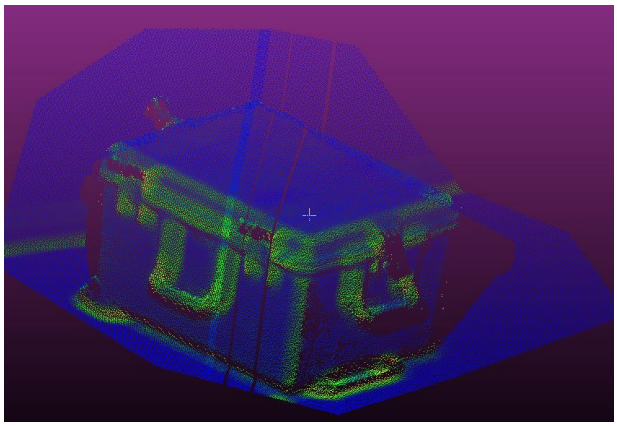

Figure 3. TLS Data According to Surface Normal (Leica C10)

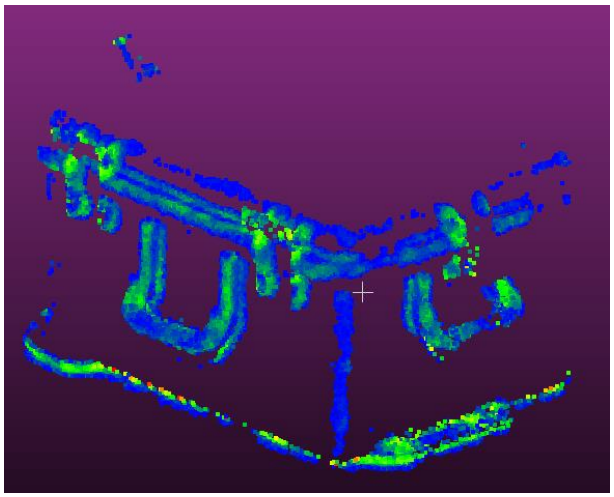

Figure 3a. Boundary and corner lines according to Surface Normal

As seen above, boundary points and corner points, which can be used in many studies, can be obtained by surface analysis (Figure 2a and Figure 3a). After these analysis, lines can be drawn automatically from the obtained points used in surveying and restoration works. On the other hand, specific primitive shapes can be extracted from point clouds to use in different engineering studies. For this purpose, the RANSAC algorithm have been tested in this study by using the Cloud compare program. Obtained results are presented at Figure 4. Locally fitting primitives like planes, cylinders, and cones using RANSAC-based algorithms is a popular. As seen from this case study, since there are only plane surfaces, the other cylinder, sphere etc. this application could not be tested either.

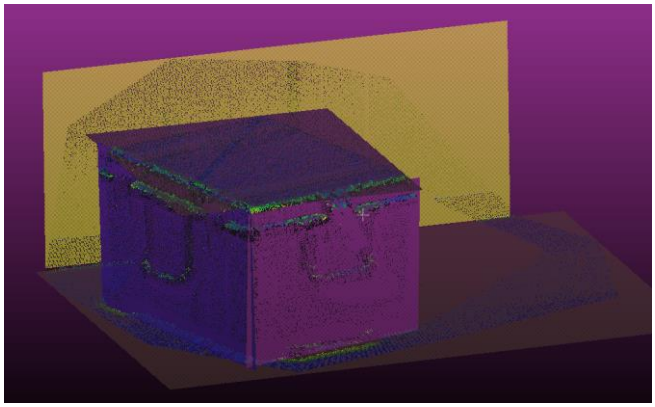

Figure 4. The primitive shapes (planes) with RANSAC Algorithm for small point cloud data

According to the results obtained from the studies with the RANSAC algorithm, the performance of the RANSAC algorithm in big data has been tested. Since there are only plane features in the case study data, plane surfaces can be obtained accurately in extensive data as follows (Figure 5).

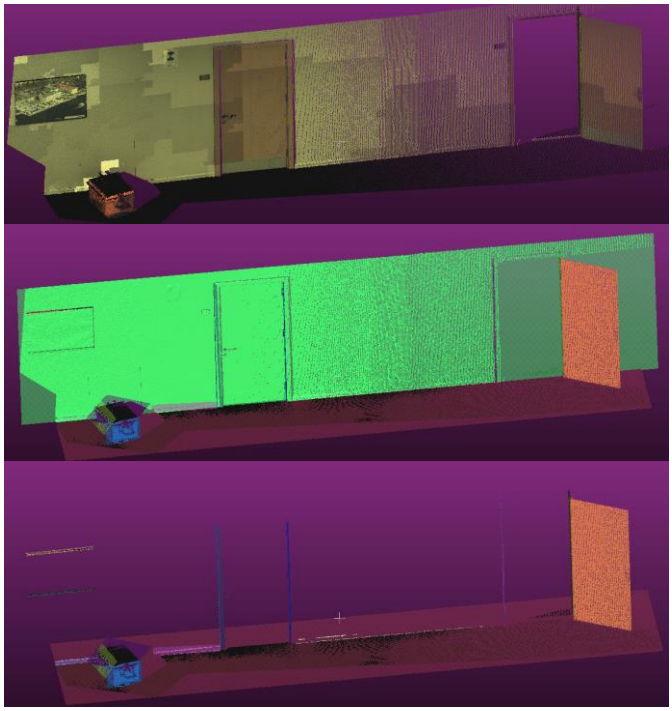

Figure 5. The primitive shapes (planes) with RANSAC Algorithm for dense point cloud

As seen in Figure 5, it is the topmost original point cloud. The figure in the middle is RANSAC applied. In the middle picture, the algorithm could extract the walls and doors clearly as a plane. The bottom picture can be seen that it can extract the plane surfaces of the doors and the painting on the wall. According to the results above, the RANSAC algorithm can easily extract plane surfaces on LiDAR data.

In this study, Total station measurements also were made to determine the accuracy of the laser point clouds. The accuracy of the laser point clouds was calculated by taking the differences from about ten distances at specific points (Table 1). TLS data was found to have a standard deviation of 0.007 m.

Table 1. The base distances of points and the differences

Points (m)	Total_Station	Lazer	Diffrence (m)
23-22	5.496	5.490	0.005
23-21	6.551	6.542	0.008
23-20	4.554	4.557	-0.002
23-19	4.657	4.635	0.021
22-21	1.694	1.697	-0.002
22-20	2.660	2.655	0.005
22-19	4.783	4.775	0.007
21-20	4.315	4.312	0.002
21-19	4.516	4.509	0.007
20-19	6.180	6.168	0.012

4. DISCUSSION

For architecture projects, terrestrial laser scanning data can be edited in various CAD systems. This research aims to perform a 3D analysis of a building scanned with 3D terrestrial laser scanning technology. After analyzing object features with a terrestrial laser scanner, RANSAC Algorithm was used to construct 3D models and 3D surfaces from 3D point clouds. The benefits and drawbacks of open source code software are also being assessed for getting 3D surfaces and doing various surface analyses utilizing an Open Source program.

Statistical methods were used to compare the base distances, and the coarse mistakes were removed from both sets of data. For TLS, the standard deviation of the base distances was computed. TLS data was found to have a standard deviation of 0.007 m. All standard deviations of the 3D models are acceptable; compared with the data accuracy acquired by the scanner of Leica.

Point cloud resolution and accuracy are critical to building 3D precise mesh models and surface characteristics. As a result, working with high resolution and accuracy point clouds rather than additional point clouds in 3D modeling is the foundation of research in point clouds. As a result, it is critical to use high-precision point clouds, plenty of them for data modeling. Various filtering algorithms can be used for modeling, interpolation, and surface fitting operations; however, modeling or interpolating data that is missing or wrongly measured is always challenging. The results show that the RANSAC Algorithm can produce high-precision and complete three-dimensional geometric models, resulting in reliable 3D data that is important for restoration and other engineering works.

5. CONCLUSION

Working with high-accuracy points to model point clouds and having enough data is a critical aspect of point cloud research. In point cloud investigations, it is also crucial to know the precision or resolution required for modeling. The registration or modeling processes can be completed if the point clouds are sufficient for the desired works. If the needed surface data is absent or of insufficient precision and resolution in the existing point cloud, it will be a more accurate technique to create a more accurate point cloud from the existing point cloud and integrate it into the reference data for interpolation or modeling.

The experiments performed in this study show that one unique technique or geometric features cannot recommendable for the 3D Surface parameters or 3D models of 3D point cloud. In the process of surface reconstruction, Random Sample Consensus (RANSAC) is frequently applied. Geometric features of point clouds produced at multi scales can be used for vertices and boundary lines from 3D point clouds.

Acknowledgements

The preliminary results of this study were presented at *4th Intercontinental Geoinformation Days (IGD) – 20-21 June 2021 – Tabriz, Iran.* Also, thanks to everyone who contributed to using the Leica C10 laser scanner, which belongs to the ITU Geomatics Engineering Department, and bringing it to the department.

Author contributions

The authors contributed equally.

Conflicts of interest

There is no conflict of interest between the authors.

Statement of Research and Publication Ethics

The authors declare that this study complies with Research and Publication Ethics

References

Almagro, A. & Almagro, V. A. (2007). Traditional Drawings Versus New Representation Techniques. The ISPRS International Archives of the Photogrammetry, Remote Sensing and Spatial Information Sciences, Athens, Greece, Vol. XXXVI5/C53, pp. 52-57

Alptekin, A. & Yakar, M. (2020). Mersin Akyar Falezi'nin 3B modeli. Türkiye Lidar Dergisi, 2(1), 5-9.

Alptekin, A., Çelik, M. Ö. & Yakar, M. (2019a). Anıtmezarın yersel lazer tarayıcı kullanarak 3B modellenmesi. Türkiye Lidar Dergisi, 1(1), 1-4.

Alptekin, A., Fidan, Ş., Karabacak, A., Çelik, M. Ö. & Yakar, M. (2019b). Üçayak Örenyeri'nin yersel lazer tarayıcı kullanılarak modellenmesi. Türkiye Lidar Dergisi, 1(1), 16-20.

Altuntas, C., Yildiz, F., Karabork, H., Yakar, M. & Karasaka, L. (2007, October). Surveying and documentation of

detailed historical heritage by laser scanning. In XXI International CIPA Symposium (Vol. 1, No. 06).

Atik, M. E., Duran, Z. & Seker, D. Z. (2021). Machine learning-based supervised classification of point clouds using multiscale geometric features. *ISPRS International Journal of Geo-Information*, *10*(3), 187.

Çelik, M. Ö., Hamal, S. N. G. & Yakar. İ. (2020). Yersel Lazer Tarama (YLT) Yönteminin Kültürel Mirasın Dokümantasyonunda Kullanımı: Alman Çeşmesi Örneği. Türkiye LiDAR Dergisi, 2 (1), 15-22.

Fischler, M. A. & Bolles, R. C. (1981). Random sample consensus: a paradigm for model fitting with applications to image analysis and automated cartography. Communications of the ACM, Vol. 24(6), pp. 381-395.

Foorginejad, A. & Khalili, K. (2014). Umbrella curvature: a new curvature estimation method for point clouds. *Procedia Technology, 12*, 347-352.

Fowler, A. & Kadatskiy, V. (2011). Accuracy and error assessment of terrestrial, mobile and airborne LiDAR. Paper presented at the Proceedings of American Society of Photogrammetry and Remote Sensing Conference (ASPRP 2011), 1–5 May 2011, Milwaukee, Wisconsin.

Grilli, E., Menna, F. & Remondino, F. (2017). A review of point clouds segmentation and classification algorithms. *The International Archives of Photogrammetry, Remote Sensing and Spatial Information Sciences*, *42*, 339.

He, B., Lin, Z. & Li, Y. F. (2013). An automatic registration algorithm for the scattered point clouds based on the curvature feature. *Optics & Laser Technology, 46*, 53-60.

Hoppe, H., DeRose, T., Duchamp, T., McDonald, J. & Stuetzle, W. (1992). *Surface reconstruction from unorganized points* (Vol. 26): ACM.

Korumaz, S. A. G. (2021). Terrestrial Laser Scanning with Potentials and Limitations for Archaeological Documentation: a Case Study of the Çatalhöyük. *Advanced LiDAR*, *1*(1), 32-38.

Kuçak, R. A., Kılıç, F. & Kısa, A. (2014). Analysis Of Various Data Collection Methods For Documentation Ofhistorical Artifacts. Paper presented at the 5. Remote Sensing-GIS Conference , İstanbul.

Kuçak, R., Erol, S. & İşiler, M. (2020). The Accuracy Assessment of Terrestrial and Mobile LiDAR Systems for 3D Modelling. Proceedings book of the 1st Intercontinental Geoinformation Days (IGD) Symposium, Mersin, Mersin, Turkey.

Kuçak, R., Kılıç, F. & Kısa, A. (2016). Analysis of terrestrial laser scanning and photogrammetry data for documentation of historical artifacts. The International Archives of Photogrammetry, Remote Sensing and Spatial Information Sciences, 42, 155.

Kuçak, R., Özdemir, E. & Erol, S. (2017). The segmentation of point clouds with k-means and ANN (artifical neural network). The International Archives of Photogrammetry, Remote Sensing and Spatial Information Sciences, 42, 595.

Li, M., Jinming, Z., Dongchao, M. & Yingxun, F. (2019). An Improved RANSAC Surface Reconstruction Study. In *Journal of Physics: Conference Series* (Vol. 1284, No. 1, p. 012020). IOP Publishing.

Liu, J. (2020). An adaptive process of reverse engineering from point clouds to CAD models. *International Journal of Computer Integrated Manufacturing*, *33*(9), 840-858.

Pauly, M., Gross, M. & Kobbelt, L. P. (2002). *Efficient simplification of point-sampled surfaces.* Paper presented at the Proceedings of the conference on Visualization'02.

Schnabel, R., Degener, P. & Klein, R., (2009). Completion and reconstruction with primitive shapes. CGF Eurographics, Vol. 28(2), pp. 503-512

Ulvi, A. & Yakar, M. (2014). Yersel Lazer Tarama Tekniği Kullanarak Kızkalesi'nin Nokta Bulutunun Elde Edilmesi ve Lazer Tarama Noktalarının Hassasiyet Araştırması. Harita Teknolojileri Elektronik Dergisi, 6(1), 25-36.

Ulvi, A., Yakar, M., Toprak, A. S., & Mutluoglu, O. (2014). Laser Scanning and Photogrammetric Evaluation of Uzuncaburç Monumental Entrance. International Journal of Applied Mathematics Electronics and Computers, 3(1), 32-36.

Yakar, M., Yılmaz, H. M. & Mutluoğlu, H. M. (2009). Hacim Hesaplamalarında Laser Tarama ve Yersel Fotogrametrinin Kullanılması, TMMOB Harita ve Kadastro Mühendisleri Odası 12. Türkiye Harita Bilimsel ve Teknik Kurultayı, Ankara.

Yakar, M., Yilmaz, H. M. & Mutluoglu, O. (2014). Performance of Photogrammetric and Terrestrial Laser Scanning Methods in Volume Computing of Excavtion and Filling Areas. Arabian Journal for Science and Engineering, 39(1), 387-394.

Yılmaz, H. M. & Yakar, M. (2006a). Lidar (Light Detection And Ranging) Tarama Sistemi. Yapı Teknolojileri Elektronik Dergisi, 2(2), 23-33.

Yılmaz, H. M. & Yakar, M. (2006b). Yersel lazer tarama Teknolojisi. Yapı teknolojileri Elektronik dergisi, 2(2), 43-48.

© Author(s) 2022.
This work is distributed under https://creativecommons.org/licenses/by-sa/4.0/

Advanced LiDAR

http://publish.mersin.edu.tr/index.php/lidar/index

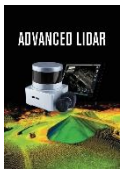

Deviation Analysis of Historical Building Based on Terrestrial Laser Scanner Data and 3D Mesh Model

S. Armağan Güleç Korumaz*[1], Recep Sayar[2]

[1] *Konya Technical University, Faculty of Architecture and Design, Konya, Turkey*
[2] *MSc, Architect*

Keywords
Cultural Heritage,
Deviation Analysis,
Point Cloud,
Terrestrial Laser Scanning.

ABSTRACT

The use of Terrestrial Laser Scanner (TLS) technologies in cultural heritage studies has become more common day by day. In addition to documenting a historical building with high accuracy, TLS technologies can obtain detailed data about the structure being studied by analyzing point cloud. Laser scanning data is seen as a non-contact and effective analysis method in determining the formal deformations that occur due to various reasons, especially in historical buildings. With this method, it is possible to determine how much the object deviates from a reference 3D model or plane and with this analysis, deformation maps can be prepared. With the help of these maps, intervention decisions can be made. Within the scope of the article, laser scanning data of Selime Sultan Tomb located in Güzelyurt Selime Town in Türkiye, one of the important settlements of Cappadocia, were acquired. By comparing the 3D mesh model prepared with base on point data, the morphological differences and deviations of the tomb were determined and mapped.

1. INTRODUCTION

In the last 20 years, laser scanning technologies have brought new initiatives to cultural heritage studies. Laser scanning data is used to define the structural safety of historical buildings and to determine their formal anomalies. Laser scanning technology collects highly accurate 3D data to provide conceptual understanding of the historic building (Lindenbergh, R., & Pietrzyk, P. 2015). By analyzing the laser scanning data, information of the possible behavior of the buildings could be obtained. (Fregonese et al., 2013; Kaartinen, 2022; Alptekin and Yakar., 2020, Alptekin et al., 2019a, Alptekin et al., 2019b). Moreover, using these data, the application errors related to construction period of historical building could be analyzed. Beside these, the formal deformations exposed to any reason could be determined. In addition, material properties of the building, deformations caused by the ground and the damages caused by the earthquake could be analyzed. While these analyzes are carried out in classical methods by directly contacting the surface and by establishing a scaffold, thanks to laser scanning data similar analyzes could be performed without contacting these surfaces. However, it can be said that the analyzes made with the classical methods are more subjective than the laser scanning data (Pesci et al. 2011; Altuntas et al., 2007; Ulvi and Yakar, 2014, Ulvi et al., 2014).

In recent years, quality controls could be made by using point cloud data at different stages of all production sectors. Thanks to software using point cloud data in different sectors, quality controls could be made by comparing the current sample with a reference product. Due to the benefits of this technique, different software have tried to produce solutions for the subject. In general, commercial (Geomagic, Cyclone, PolyWorks 3DReshaper etc.) and opensource software such as CloudCompare can perform these analyzes in a qualified manner.

Besides regular contact and contactless structural analysis, deviation analysis method can provide some data about the structural problems of the building and can detect the error and error resources in modelling process. Different deviation pattern could be correlated with different type of errors and deviation patterns facilitate identifying of error resources.

*Corresponding Author

*(sagkorumaz@ktun.edu.tr)ORCID ID 0000-0001-6337-9087
(recepsayar3@gmail.com) ORCID ID 0000-0002-3792-3832

Cite this;

Korumaz, G. A. S. & Sayar, R. (2022). Deviation Analysis of Historical Building Based on Terrestrial Laser Scanner Data and 3D Mesh Model. Advanced LiDAR, 2(1), 21-30.

Research Article

Accepted: 27/03/2022

2. DEVIATION ANALYSIS

The term deviation, which is used by different disciplines, is a method of determining differences and anomalies by making comparisons from a plane or object at a certain time or periodically in production or construction industry. According to Anil et. al. (2013) TLS data base analyses 6 times more sensitive than eye-contact observations.

These analyses techniques could be carried out by different data or 3D model for different purpose:

- *Comparison of two point clouds at different times:* Generally, this comparison purposes as an observation of building Deviations from the reference point cloud by comparing point clouds measured at different times (Scaioni, 2013; Wunderlich, 2016). Similarly, point clouds from different sources could be compared (Ahmad Fuad,2018; Vanneschi et. all, 2017; Yakar et al., 2009, Yakar et al., 2014, Yılmaz and Yakar., 2006a). These sources can be photogrammetric data and TLS data or point clouds could be obtained with different devices. In this technique, the main challenge is how to efficiently and precisely identify the correspondences points between the compared objects.

- *Deviation analysis of building with respect to orthogonal planes:* They are widely used for vertical deviations of tall buildings or for deformation mapping of surfaces. Thanks to laser scanner data some deformations could be measured about the historical buildings like overhanging of some part of building, progressive changes of inclinations, differential movement of structure (Castagnetti et.al. 2012). Deviations have been defined by carrying out a detailed analysis of deflection from verticality with respect to orthogonal plane that is perpendicular position of the inclination direction. Vertically analysis of high buildings can be carried out by cutting point cloud or mesh models and obtained sections. (Bertacchini et. al.2010). This method can provide data local leaning and tapering angle, radius, local deviations from local curvatures (Teza and Pesci 2013). Similarly, deformation maps can be created on large surfaces by measuring their distances relative to a reference coordinate system or reference plane. The main difficulty in this method is how to create and determine the reference plane and the location related to the building. Essentially, a point on a building that is assumed to remain unchanged over time can form the reference point of the reference plane.

-*Surface analysis of building with best-fit cone and cylinder or 3D Model:* Some software packages are optimized for analysis of mesh and point cloud data as a reliable tool for shape analysis with respect to planer, spherical, cylinder and cone reference objects. (Korumaz et. al, 2017; Yang, 2017, Bruno, 2018). The computation of the distance field between the point cloud or mesh model and reference shapes provides local deviations from the expected shape

The error map-based approach can be carried out with standard tools for point cloud inspection. In many case examples, geometries that are not cones or cylinders cannot be analyzed because a single suitable geometry cannot be created for the entire object, and sometimes a different reference geometry must be created for each part of the building.

-*Point cloud versus mesh model comparisons for the whole structure:* It is the comparison of the prepared mesh model with the point cloud data of the structure (Nguyen,2018). This technique could be used in reverse engineering applications for comparing deformation of final product and prepared mesh model. In addition, by comparing an idealized mesh model with a point cloud, the deviations of the structure from this model can be measured and comments on the deviation could be made.

Deviation analysis consists of four stages:

a. Determination of deviation analysis techniques according to features of the building. The deviation analysis technique is determined according to the nature of the surface or all building to be analyzed. Comparison of different point clouds, reference plane, best fit cone or cylinder, or 3D mesh model comparisons are selected based on analysis.

It is observed in the literature that the analyzes of a tall building are mainly for deviation from the vertical plane (Schneider, 2006; Yılmaz and Yakar., 2006b). Similarly, in high-rise buildings, a reference cone, cylindrical or prismatic geometry that best overlaps with the point cloud can be compared to the whole or part of the building. More complex forms can be compared with prepared 3D models and differences could be obtained.

b. Mapping of Deviations: Thematic expression of deviations is a mapping method that the best overlapping segments are marked as green (0 and close to zero value) and positive and negative differences as from red to blue. Map colors may change according to the determination of threshold values. The smaller threshold value ranges in mapping, the more precise the damage can be expressed. As the threshold values increase, the content of the map becomes more general.

c. Deviation analysis and determination deviations' reasons: The main purpose of damage detection in cultural heritage studies is to find the source of this anomalies. Prepared deformation maps give a preliminary idea of damages (Neuner et. All, 2016; Holst, 2017). Vertical distortions, ground strength problems, anomalies on the walls, color differences, vegetation on the surface can be given as examples (Hsieh, 2012). After these determinations, the laser scanning data may not be sufficient and the causes of the deformations can be determined by using different techniques.

d. Generating intervention decisions: Intervention decisions related to cultural heritage can only be developed based on highly accurate documentation and analysis methods. One of the most important criteria for its interventions are the correct determination of the problems. Intervention decisions can be made based on these correct determinations. Structural interventions could be made according to the size of the deformation in the historical building. Soil reinforcement can be applied for ground settlements. Preventive measures for cracks, deformations and spills on flat surfaces could be made in line with the analysis.

3. METHOD

The methodology of the study consists of two parts. In the first part, the point cloud model of the Tomb is created using TLS data. The second part consists of comparing the point cloud with the idealized 3D mesh model produced with reference to the point cloud and the creation of the deformation maps. FaroS120 was used to obtain the point cloud, and post-process applications were produced in Faro Scene software. SketchUp was used for creating 3D Cad model and UNDET software was used to import the point cloud to Sketchup. Cloud Compare opensource software was used for point cloud comparison and deformation maps with produced 3d model (Figure 1).

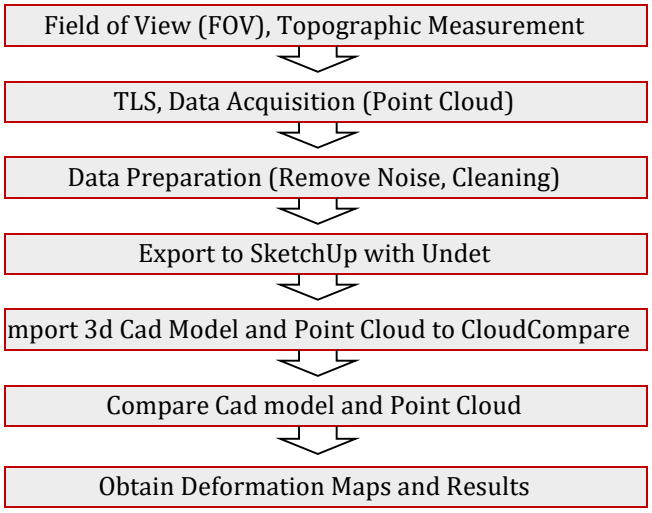

Figure 1. Workflow of Study

4. DATA AQUSITION, POST PROCESSING and DEVIATION ANALYSIS OF HISTIRICAL TOMB

4.1. Short History of Tomb

The tomb is in the borders of the Cappadocia region within Aksaray province in Turkey. It is mentioned as Ali Pasha Tomb (Konyalı, 1975), Anonymous Tomb (Bakırer, 1981), Selime Hatun Tomb (Anonymous, 1995), Selime Sultan Tomb (Önkal, 1996) in researches and various publications (Figure 2,3). Although the exact date of construction of the tomb is not known, researchers generally dated its construction period as XIII century. The building was abandoned for many years and its restoration was carried out in 1996. The building consists of two floors. The burial space is located in the basement level and there are symbolic mausoleums in the upper part.

It is observed that it was exposed to severe deformations with examination of old pictures of the building (Figure 4-5). Major interventions or repairs were made in restoration process in 1996. The tomb has an octagonal plan scheme. This octagonal plan narrows towards the upper levels and the surfaces are inclined. Constructing this geometry requires very careful craftsmanship. Within the scope of the article, analyzes were made to determine whether this geometry was restored properly or not.

Figure 2. Current Images of Tomb

Figure 3. Entrance of Tomb and Brick Array

Figure 4. Old images of Tomb before 60's.

Figure 5. Structural deformations of Tomb around 60's.

4.2. Data Acquisition

Data acquired with Terrestrial Laser Scanner (Faro S120 Laser Scanner) were transferred and aligned with Faro Scene software. All alignment, flittering, cleaning works carried out in Scene software. The building was scanned in the form of two intertwined circular path. While the far scans measure the cone section of the tomb, the scans in the inner circle are close to the octagonal façade of the tomb and intensive measurements were made. During the scanning, positions were chosen providing a perpendicular angle to the surface for reducing distorted number of the points. In the post-processing stage, a more homogeneous point cloud was obtained by cleaning and filtering of the dataset separately for each scan. After this stage, approximately 22 thousand points remain after filtering and subsampling (Figure 6).

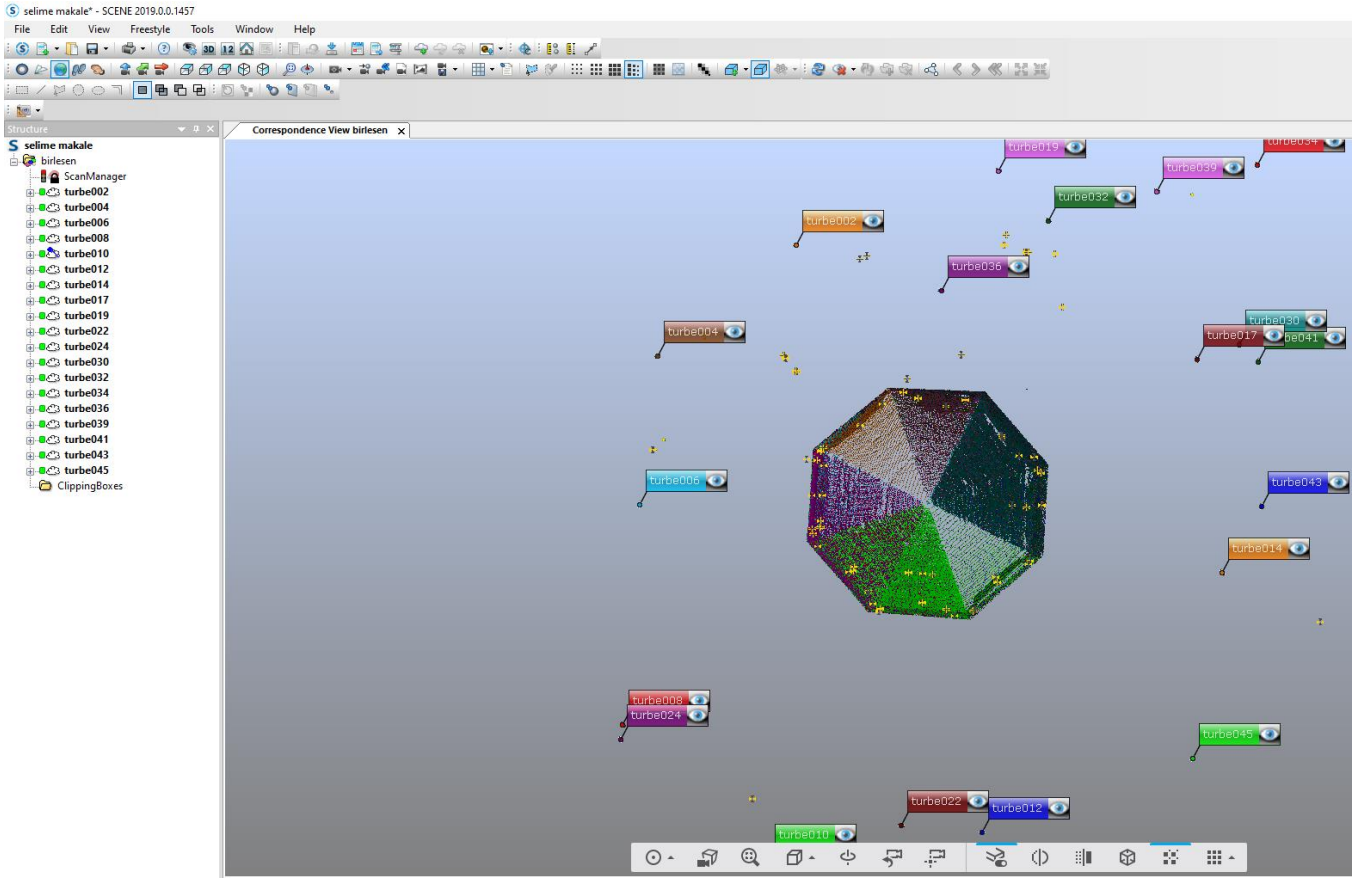

Figure 6. After postprocessing of Tomb's data in Faro Scene.

4.2. 3D Cad Modeling of Tomb

The point cloud was exported in E57 format. The extracted point cloud was imported into SketchUp using the Undet plugin. Undet Plugin was used while importing the point cloud into the Sketch Up. Undet plugin provide to point cloud to be managed and organize point cloud. Thanks to this plug in it is possible to measure distances and vertical and horizontal sections could be prepare for CAD modeling of building. Undet plugin also provide snapping of point cloud. This is very helpful for creating 3D cad model in Sketch Up. Preliminary comparison of the prepared 3d mesh model and the point cloud is made in Sketch Up and User was able to observe the differences between the model and the point cloud (Figure 7-8).

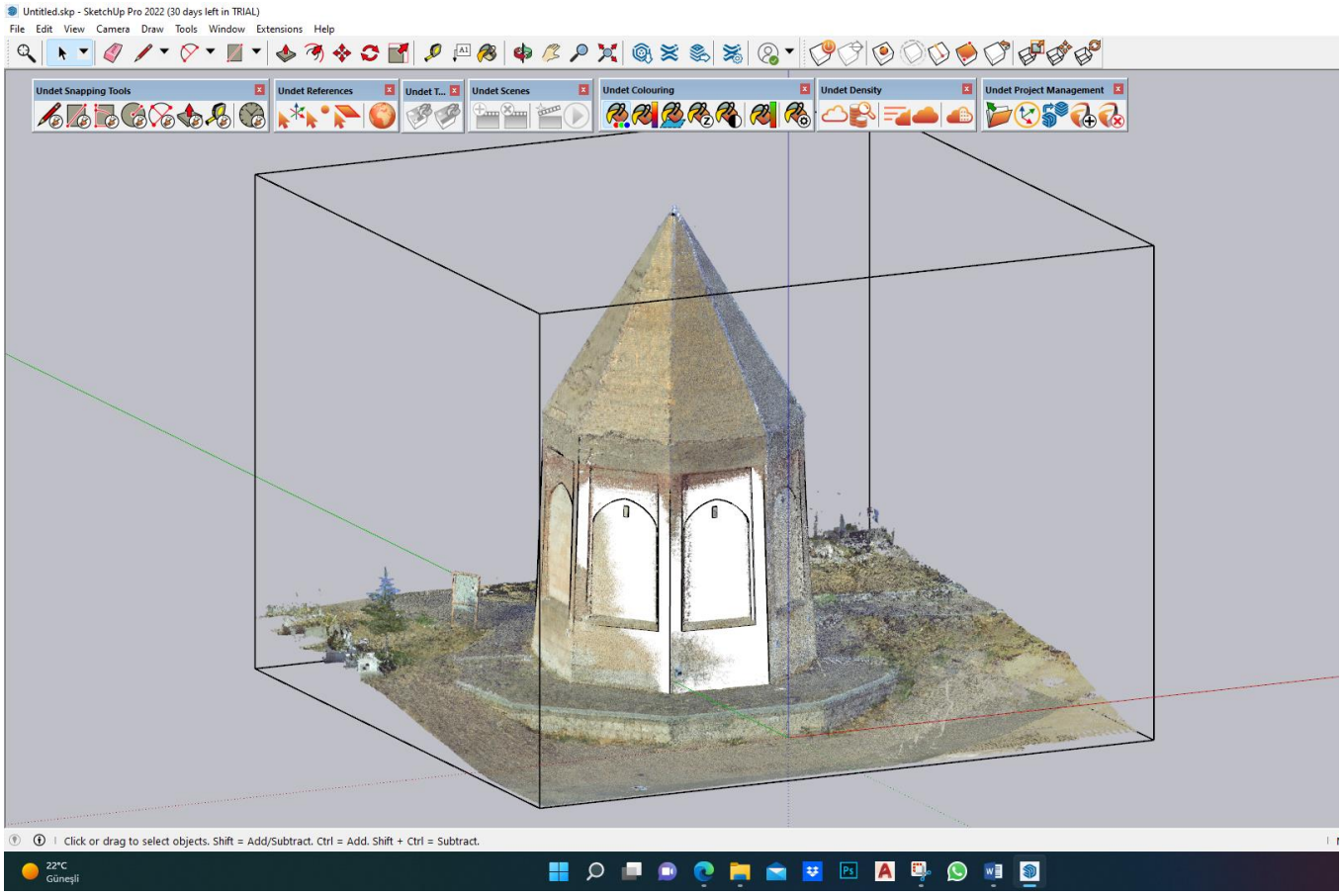

Figure 7. Point Cloud and 3D Mesh Model in Sketch Up.

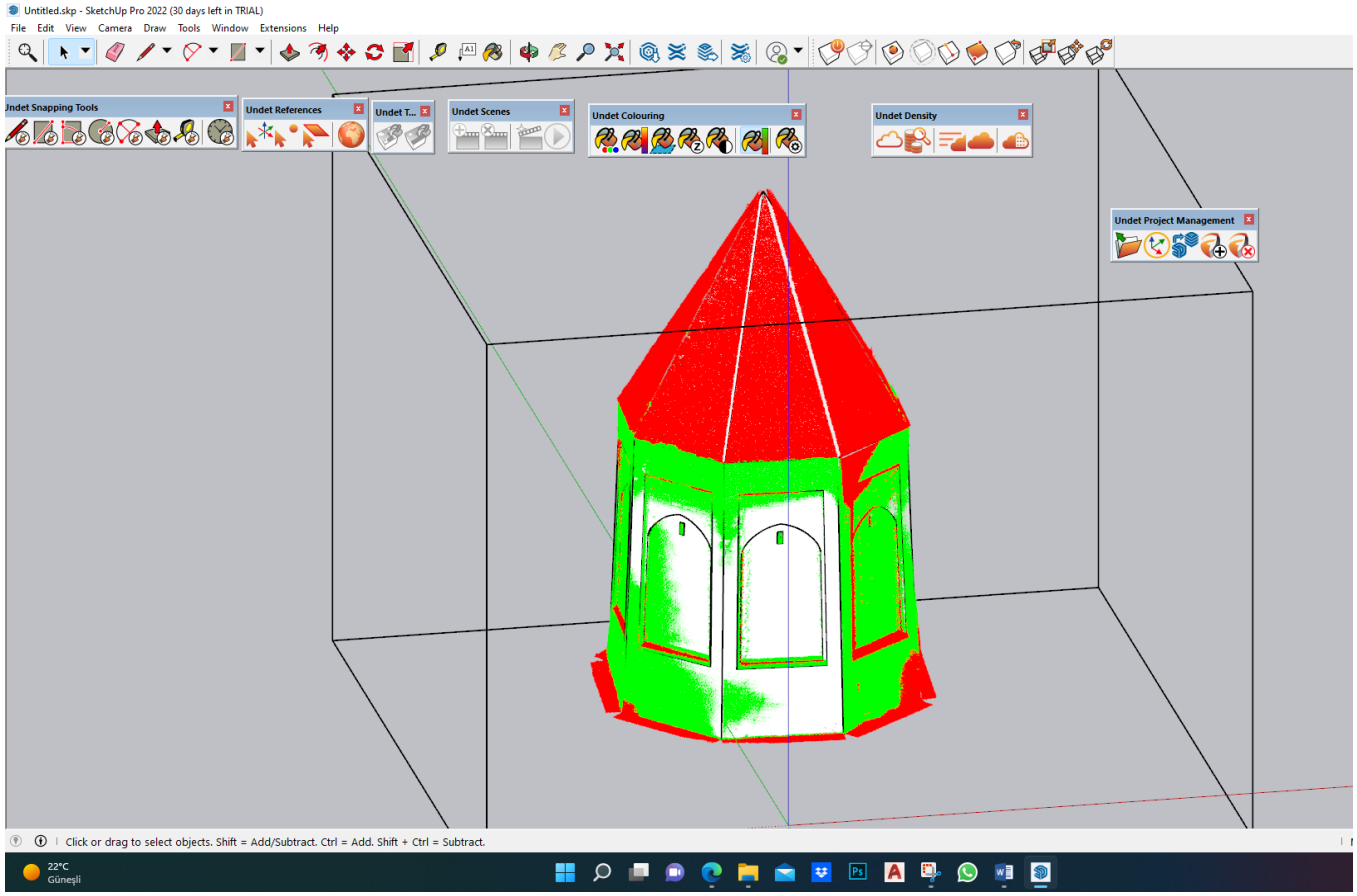

Figure 8. Pre-comparison of point cloud and 3d model in Sketchup with Undet Plugin.

4.4. Comparison of Point Cloud and 3D Mesh Model

CloudCompare is an opensource software for any purpose commercial and education. This software provides significant advantages regarding point cloud postprocessing. The most important of these advantages is the comparison of two point cloud data and mapping according to the distance differences between them. In addition, a reference mesh model and reference plane can be compared with the point cloud. The mesh model and point cloud prepared within the scope of the study were imported into CloudCompare and comparisons were made. It should be considered at this stage is to the overlap of the cloud data and the boundaries of the 3D model. In this context, if deformed points and parts that need to be filtered are observed in the point cloud, these areas must be segmented (after segmentation unnecessery point cloud could be delate) or filter could be applied. At this step, the pointcloud data density could be reduced by sampling so that the point cloud density could be homogeneous. Within the scope of the study, noise filter was applied to the point cloud data and then a homogeneous point cloud was obtained by sampling at 0.005m intervals. After this application, the point cloud, which was around 55 million, decreased to around 22 million (Figure 9-10).

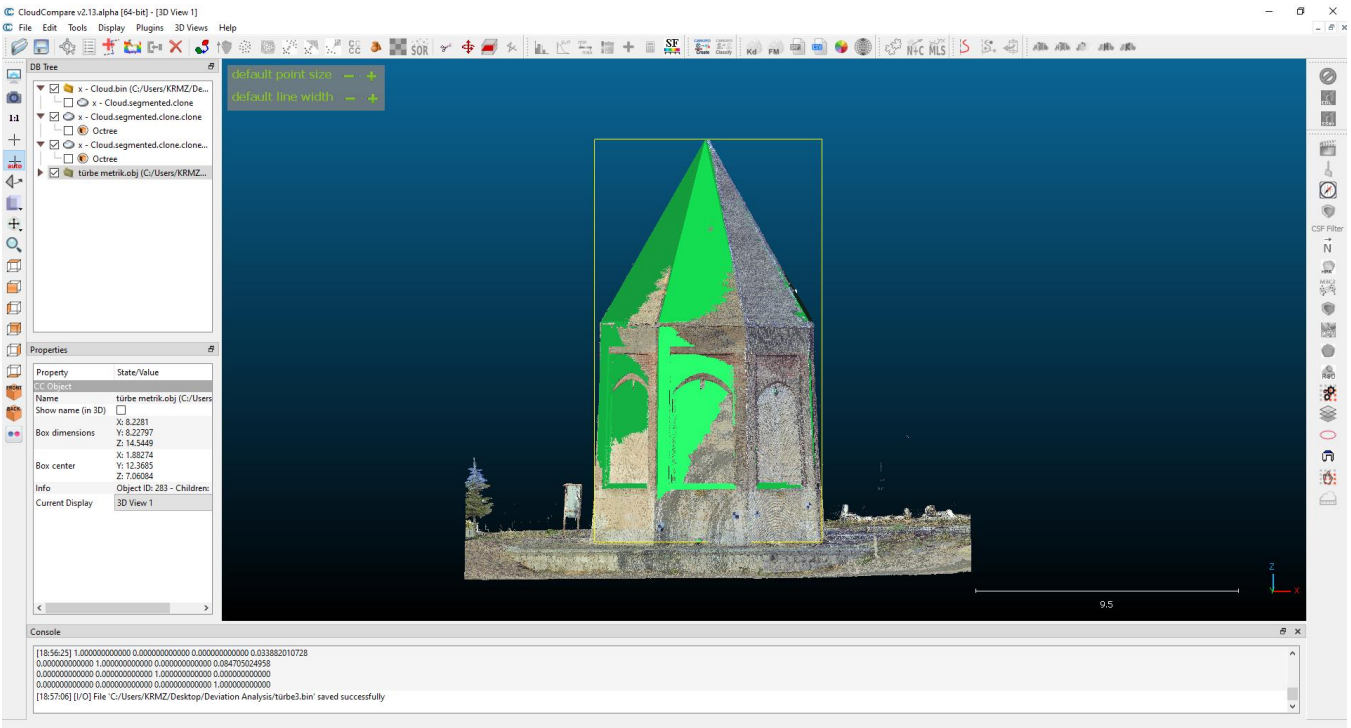

Figure 9. Point Cloud and 3D Mesh model in CloudCompare

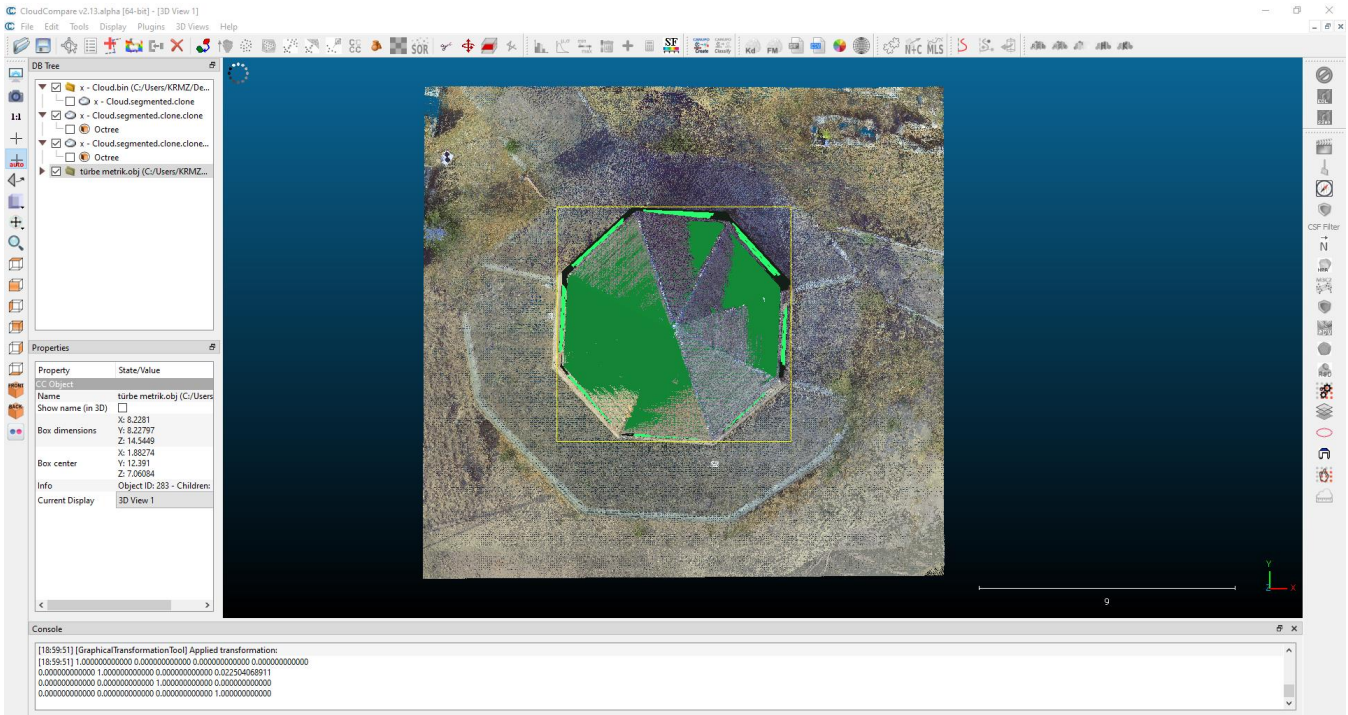

Figure 10. Point Cloud and 3D Mesh model in CloudCompare

After these preparations, the point cloud and the mesh model were compared. In the preliminary comparison, the software makes a pre-evaluation. In this evaluation, 3D mesh model is automatically used as the reference object. For cloud to mesh comparison, these parameters were chosen: Octree level: this is the level of subdivision of the octrees at which the distance computation will be performed. In this article octree level was used as default setting. Signed distance, flip normal and multi-threaded adjustments are used as default setting as well (Figure 11). After the analysis was completed, the results obtained were expressed graphically. In this study, the Cloud to Mesh "*Signed distance*" was determined between +0.3m and -0.3m. The color range of the deformation range is expressed in the display parameter range chart. The most intense color difference in this diagram is used in the deformation map (Figure 12).

As a result of the comparison, it has been observed that the geometry of the tomb differs from the targeted geometry (3d Mesh model) in the first time period and there are slope differences between the surfaces. The surface slopes of the cone and the tomb is different from each other. This difference shows that the tomb was deformed in form within the restorations made in 1996. It shows that the deformation of the sections closes to shades of green on the thematic maps is less than 0.15m. It has been observed that there are more distance differences of more than 0.15m in the red sections. While the biggest differences in the facades were in the entrance facade, it was observed that the differences in the right side and left side facades were less than 0.15m (Figure 13-16).

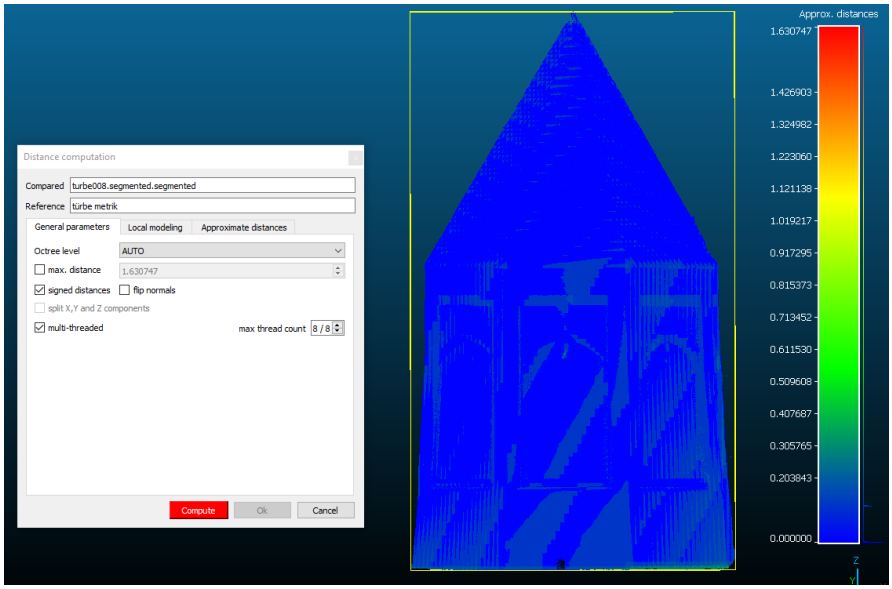

Figure 11. Pre-comparison of Point Cloud and Mesh Model

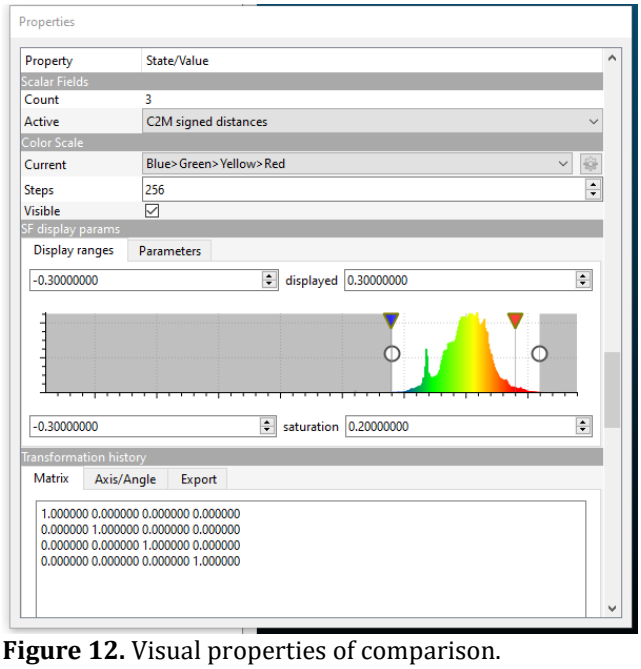

Figure 12. Visual properties of comparison.

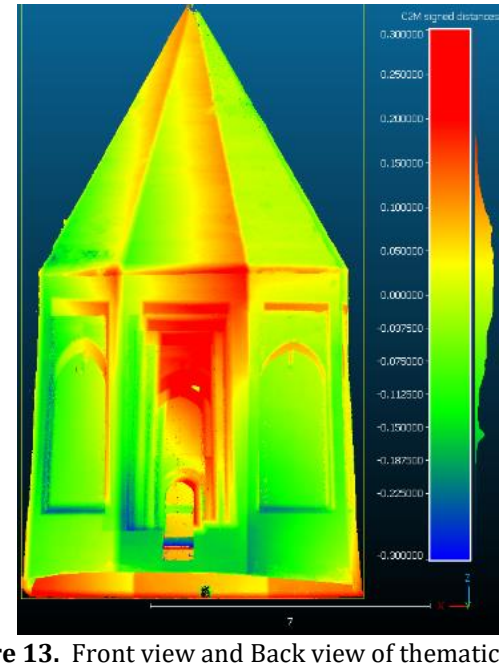

Figure 13. Front view and Back view of thematic map.

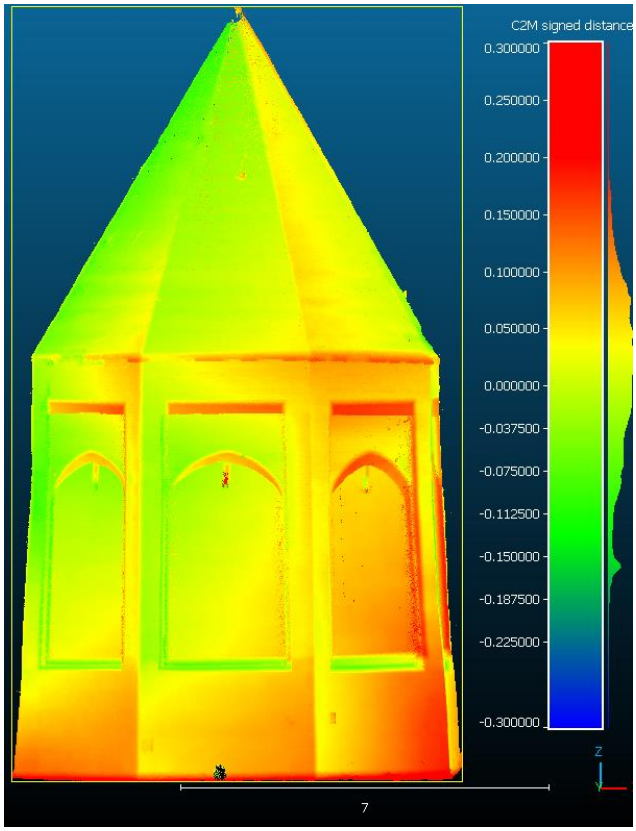

Figure 14. Front view and Back view of thematic map.

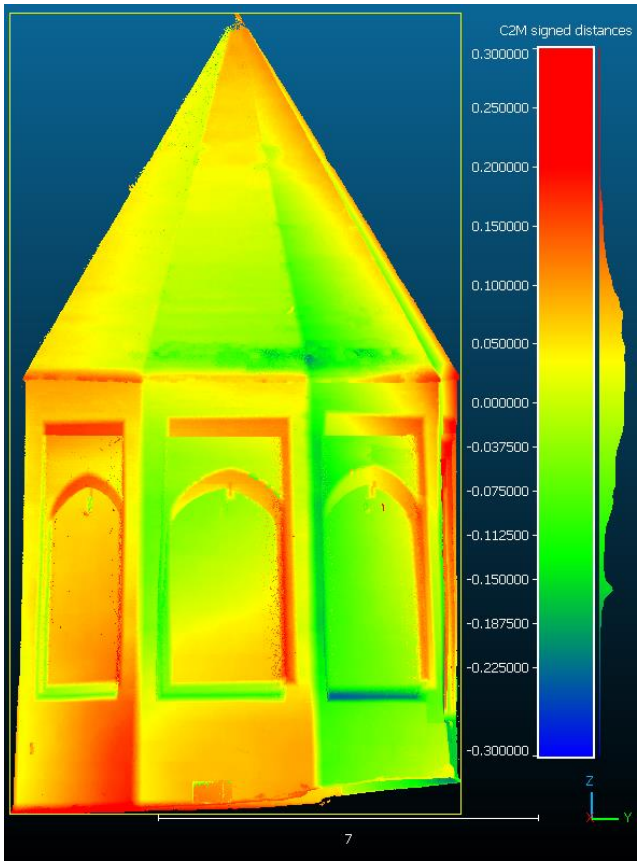

Figure 15. Right view and left view of thematic map.

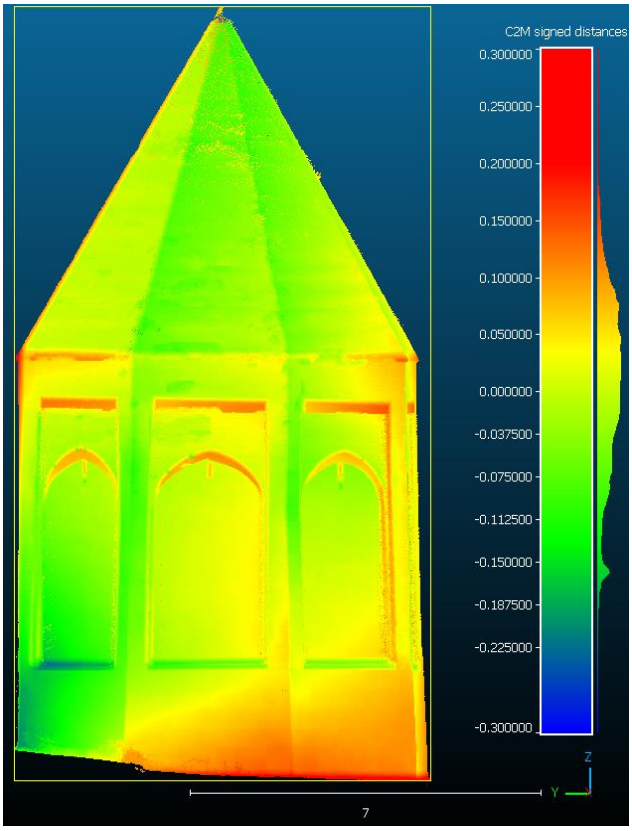

Figure 16. Right view and left view of thematic map.

5. RESULTS

In this article, the results are shared that obtained by comparing point cloud data and 3D mesh model. Deviation analysis method gives an idea of how much difference occurs from ideal reference geometry by comparing point cloud data. These differences could be arisen from the time period when the building was first built, as well as natural disasters, ground and material problems over time.

In the case of Aksaray Selime Sultan Tomb, the historical building was abandoned for a long time, and the building was almost rebuilt with an insensible restoration work in 1996. During the restoration, it was observed that there were formal deformations on the structure, its geometry was disturbed, and there were different slopes on the vertical and lateral surfaces. It is understood that the cone shape deviates from the central point.

This case study is important in terms of identifying restoration errors as a result of comparing the point cloud, which develops an innovative analysis method in cultural heritage studies, with a reference plane and object. An intervention decision for the deformations with the thematic maps obtained from the study could be suggested by the restorer architects or structural engineers.

Author contributions

The authors contributed equally.

Conflicts of interest

There is no conflict of interest between the authors.

Statement of Research and Publication Ethics

The authors declare that this study complies with Research and Publication Ethics

References

Ahmad Fuad, N., Yusoff, A. R., Ismail, Z. & Majid, Z. (2018). Comparing the performance of point cloud registration methods for landslide monitoring using mobile laser scanning data. *Int. Arch. Photogramm. Remote Sens. Spat. Inf. Sci*, *42*, 11-21.

Alptekin, A. & Yakar, M. (2020). Mersin Akyar Falezi'nin 3B modeli. Türkiye Lidar Dergisi, 2(1), 5-9.

Alptekin, A., Çelik, M. Ö. & Yakar, M. (2019a). Anıtmezarın yersel lazer tarayıcı kullanarak 3B modellenmesi. Türkiye Lidar Dergisi, 1(1), 1-4.

Alptekin, A., Fidan, Ş., Karabacak, A., Çelik, M. Ö. & Yakar, M. (2019b). Üçayak Örenyeri'nin yersel lazer tarayıcı kullanılarak modellenmesi. Türkiye Lidar Dergisi, 1(1), 16-20.

Altuntas, C., Yildiz, F., Karabork, H., Yakar, M. & Karasaka, L. (2007, October). Surveying and documentation of detailed historical heritage by laser scanning. In XXI International CIPA Symposium (Vol. 1, No. 06).

Anil, E. B. (2013). Deviation analysis method for the assessment of the quality of the as-is Building Information Models generated from point cloud data." *Automation in construction* 35, 507-516.

Anonim, Aksaray Turizm Envanteri (1995). Konya, 1995, s. 17.

Bakırer, Ö. (1981). Selçuklu öncesi ve Selçuklu dönemi Anadolu mimarisinde tuğla kullanımı (Vol. 2). Orta Doğu Teknik Üniversitesi.

Bertacchini, E., Boni, E., Carpa, A., Castegnetti, C. & Dubbini, M. (2010). Terrestrial Laser Scanner for Surveying and Monitoring Middle Age Towers, FIG Congress, Facing the Challenges-Building the Capacity, Sydney, Australia.

Bruno, N. & Roncella, R. A. (2018). Restoration oriented HBIM system for cultural heritage documentation: the case study of Parma cathedral. In: The International Archives of the Photogrammetry, Remote Sensing and Spatial Information Sciences, Vol. XLII-2, 171-178.

Castagnetti, C., Bertacchini, E., Capra, A. & Dubbini, A. (2012). Terrestrial Laser Scanning for Preserving Cultural Heritage: Analysis of Geometric Anomalies for Ancient Structures. FIG Working Week 2012 Knowing to Manage the Territory, Protect the Environment, Evaluate the Cultural Heritage., Rome, Italy, 1-13

Fregonese, F., Barbieri, G., Biolzi, L., Bocciarelli, M., Frigeri, A. & Taffurelli, A. (2013). Surveying and Monitoring for Vulnerability Assessment of an Ancient Building. Sensors, 13, 9747-9773.

Holst, C., Klingbeil, L., Esser, F. & Kuhlmann, H. (2017, October). Using point cloud comparisons for revealing deformations of natural and artificial objects. In 7th International Conference on Engineering Surveying (INGEO) (pp. 18-20).

Hsieh, C. T. (2012, November). An efficient development of 3D surface registration by Point Cloud Library (PCL). In 2012 International Symposium on Intelligent Signal Processing and Communications Systems (pp. 729-734). IEEE.

Kaartinen, E., Dunphy, K. & Sadhu, A. (2022). LiDAR-Based Structural Health Monitoring: Applications in Civil Infrastructure Systems. Sensors, 22(12), 4610.

Konyalı, İ. H. (1975). Âbideleri ve kitabeleri ile Niğde Aksaray tarihi. Fatih Yayınevi.

Korumaz, M., Betti, M., Conti, A., Tucci, G., Bartoli, G., Bonora, V. & Fiorini, L. (2017). An integrated Terrestrial Laser Scanner (TLS), Deviation Analysis (DA) and Finite Element (FE) approach for health assessment of historical structures. A minaret case study. Engineering Structures, 153, 224-238.

Lindenbergh, R. & Pietrzyk, P. (2015). Change detection and deformation analysis using static and mobile laser scanning. Applied Geomatics, 7(2), 65-74.

Neuner, H., Holst, C. & Kuhlmann, H. (2016). Overview on current modelling strategies of point clouds for deformation analysis. Allgemeine Vermessungs-Nachrichten: AVN; Zeitschrift für alle Bereiche der Geodäsie und Geoinformation, 123(11-12), 328-339.

Nguyen, C. H. P. & Choi, Y. (2018). Comparison of point cloud data and 3D CAD data for on-site dimensional inspection of industrial plant piping systems. Automation in Construction, 91, 44-52.

Önkal, H. (1996). Anadolu Selçuklu Türbeleri (Vol. 91). Atatürk Kültür Merkezi.

Pesci, A., Casula G. & Boschi E. (2011). Laser scanning the Garisenda and Asinelli towers in Bologna (Italy): Detailed deformation patterns of two ancient leaning buildings, Journal of Cultural Heritage 12, 117–127.

Scaioni, M., Roncella, R., & Alba, M. I. (2013). Change detection and deformation analysis in point clouds. Photogrammetric Engineering & Remote Sensing, 79(5), 441-455.

Schneider, D. (2006, May). Terrestrial laser scanning for area based deformation analysis of towers and water dams. In Proc. of 3rd IAG/12th FIG Symp., Baden, Austria, May, 22-24.

Teza G. & Pesci A. (2013). Geometric characterization of cylinder-shaped structure from laser scanner data: development of an analysis tool and its use on a leaning bell tower. Journal of Cultural Heritage, 14, 411–423

Ulvi, A. & Yakar, M. (2014). Yersel Lazer Tarama Tekniği Kullanarak Kızkalesi'nin Nokta Bulutunun Elde

Edilmesi ve Lazer Tarama Noktalarının Hassasiyet Araştırması. Harita Teknolojileri Elektronik Dergisi, 6(1), 25-36.

Ulvi, A., Yakar, M., Toprak, A. S., & Mutluoglu, O. (2014). Laser Scanning and Photogrammetric Evaluation of Uzuncaburç Monumental Entrance. International Journal of Applied Mathematics Electronics and Computers, 3(1), 32-36.

Vanneschi, C., Eyre, M., Francioni, M. & Coggan, J. (2017, June). The use of remote sensing techniques for monitoring and characterization of slope instability. In ISRM European Rock Mechanics Symposium-EUROCK 2017. OnePetro.

Wunderlich, T., Niemeier, W., Wujanz, D., Holst, C., Neitzel, F. & Kuhlmann, H. (2016). Areal deformation analysis from TLS point clouds—The challenge flächenhafte deformationsanalyse aus tls punktwolken–die herausforderung. allgemeine vermessungs-nachrichten (avn), 123(11-12), 340-351.

Yakar, M., Yılmaz, H. M. & Mutluoğlu, H. M. (2009). Hacim Hesaplamalarında Laser Tarama ve Yersel Fotogrametrinin Kullanılması, TMMOB Harita ve Kadastro Mühendisleri Odası 12. Türkiye Harita Bilimsel ve Teknik Kurultayı, Ankara.

Yakar, M., Yilmaz, H. M. & Mutluoglu, O. (2014). Performance of Photogrammetric and Terrestrial Laser Scanning Methods in Volume Computing of Excavtion and Filling Areas. Arabian Journal for Science and Engineering, 39(1), 387-394.

Yang, H., Omidalizarandi, M., Xu, X. & Neumann, I. (2017). Terrestrial laser scanning technology for deformation monitoring and surface modeling of arch structures. Composite Structures, 169, 173-179.

Yılmaz, H. M. & Yakar, M. (2006a). Lidar (Light Detection And Ranging) Tarama Sistemi. Yapı Teknolojileri Elektronik Dergisi, 2(2), 23-33.

Yılmaz, H. M. & Yakar, M. (2006b). Yersel lazer tarama Teknolojisi. Yapı teknolojileri Elektronik dergisi, 2(2), 43-48.

© Author(s) 2022.
This work is distributed under https://creativecommons.org/licenses/by-sa/4.0/